

An Evolutionary Many-Objective Optimization Algorithm Using Reference-Point-Based Nondominated Sorting Approach, Part I: Solving Problems With Box Constraints

Kalyanmoy Deb, *Fellow, IEEE*, and Himanshu Jain

Abstract—Having developed multiobjective optimization algorithms using evolutionary optimization methods and demonstrated their niche on various practical problems involving mostly two and three objectives, there is now a growing need for developing evolutionary multiobjective optimization (EMO) algorithms for handling many-objective (having four or more objectives) optimization problems. In this paper, we recognize a few recent efforts and discuss a number of viable directions for developing a potential EMO algorithm for solving many-objective optimization problems. Thereafter, we suggest a reference-point-based many-objective evolutionary algorithm following NSGA-II framework (we call it NSGA-III) that emphasizes population members that are nondominated, yet close to a set of supplied reference points. The proposed NSGA-III is applied to a number of many-objective test problems with three to 15 objectives and compared with two versions of a recently suggested EMO algorithm (MOEA/D). While each of the two MOEA/D methods works well on different classes of problems, the proposed NSGA-III is found to produce satisfactory results on all problems considered in this paper. This paper presents results on unconstrained problems, and the sequel paper considers constrained and other specialties in handling many-objective optimization problems.

Index Terms—Evolutionary computation, large dimension, many-objective optimization, multicriterion optimization, non-dominated sorting, NSGA-III.

I. INTRODUCTION

E VOLUTIONARY multiobjective optimization (EMO) methodologies have amply shown their niche in finding a set of well-converged and well-diversified nondominated solutions in different two- and three-objective optimization problems since the beginning of the 1990s. However, in real-world problems involving multiple stake-holders and functionalities, there often exists many optimization problems that involve four or more objectives, sometimes demanding to have 10 to 15 objectives [1], [2]. Thus, it is not surprising that

Manuscript received June 14, 2012; revised November 13, 2012 and March 15, 2013; accepted May 23, 2013. Date of publication September 16, 2013; date of current version July 29, 2014.

K. Deb is Koenig endowed chair professor at the Department of Electrical and Computer Engineering, Michigan State University, East Lansing, MI 48824 USA (e-mail: kdeb@egr.msu.edu). URL: <http://www.egr.msu.edu/~kdeb>

H. Jain is a doctoral candidate at Indian Institute of Technology Delhi, India (e-mail: himanshu.j689@gmail.com).

Color versions of one or more of the figures in this paper are available online at <http://ieeexplore.ieee.org>.

Digital Object Identifier 10.1109/TEVC.2013.2281535

handling a large number of objectives had been one of the main research activities in EMO for the past few years. Many-objective problems pose a number of challenges to any optimization algorithm, including an EMO. First and foremost, the proportion of nondominated solutions in a randomly chosen set of objective vectors becomes exponentially large with an increased number of objectives. Since the nondominated solutions occupy most of the population slots, any elite-preserving EMO faces difficulty in accommodating an adequate number of new solutions in the population. This slows down the search process considerably [3], [4]. Second, implementation of a diversity-preservation operator (such as the crowding distance operator [5] or clustering operator [6]) becomes a computationally expensive operation. Third, visualization of a large-dimensional front becomes a difficult task, thereby causing difficulties in subsequent decision-making tasks and in evaluating the performance of an algorithm. For this purpose, the performance metrics (such as hyper-volume measure [7] or other metrics [3], [8]) are either computationally too expensive or may not be meaningful.

An important question to ask is then, “Are EMOs useful for many-objective optimization problems?” Although the third difficulty related to visualization and performance measures mentioned above cannot be avoided, some algorithmic changes to the existing EMO algorithms may be possible to address the first two concerns. In this paper, we review some of the past efforts [9]–[14] in devising many-objective EMOs and outline some viable directions for designing efficient many-objective EMO methodologies. Thereafter, we propose a new method that uses the framework of NSGA-II procedure [5], but works with a set of supplied or predefined reference points and demonstrates its efficacy in solving two-objective to 15-objective optimization problems. In this paper, we introduce the framework and restrict it to solving unconstrained problems of various kinds, such as having normalized, scaled, convex, concave, disjointed, and focusing on a part of the Pareto-optimal front. Practice may offer a number of such properties to exist in a problem. Therefore, an adequate test of an algorithm for these eventualities remains an important task. We compare the performance of the proposed NSGA-III with two versions of an existing many-objective EMO (MOEA/D [10]), as the method is somewhat similar to the proposed

method. Interesting insights about both versions of MOEA/D and NSGA-III are revealed. The proposed NSGA-III is also evaluated for its use in a few other interesting multiobjective optimization and decision-making tasks. In the sequel of this paper, we suggest an extension of the proposed NSGA-III for handling many-objective constrained optimization problems and a few other special and challenging many-objective problems.

In the remainder of this paper, we first discuss the difficulties in solving many-objective optimization problems and then attempt to answer the question posed above about the usefulness of EMO algorithms in handling many objectives. Thereafter, in Section III, we present a review of some of the past studies on many-objective optimization, including a recently proposed method [10]. Then, in Section IV, we outline our proposed NSGA-III procedure in detail. Results on normalized DTLZ test problems up to 15 objectives using NSGA-III and two versions of MOEA/D are presented in Section V-A. Results of the scaled version of DTLZ problems suggested here are shown next. Thereafter, in subsequent sections, the NSGA-III procedure is tested on different types of many-objective optimization problems. Finally, NSGA-III is applied to two practical problems, involving three- and nine-objective problems in Section VII. The conclusion of this extensive study are drawn in Section VIII.

II. MANY-OBJECTIVE OPTIMIZATION PROBLEMS

Loosely speaking, many-objective optimization problems are defined as problems with four or more objectives. Two-objective and three-objective problems fall into a different class as the resulting Pareto-optimal front and, in most cases, can be comprehensively visualized by graphical means. Although a strict upper bound on the number of objectives for a many-objective optimization problem is not so clear, except for a few occasions [15], most practitioners are interested in a maximum of 10–15 objectives. In this section, we first discuss difficulties that an existing EMO algorithm may face in handling many-objective problems and investigate if EMO algorithms are useful at all in handling a large number of objectives.

A. Difficulties in Handling Many Objectives

It has been discussed elsewhere [4], [16] that the current state-of-the-art EMO algorithms that work under the principle of domination [17] may face the following difficulties.

- 1) *A large fraction of population is nondominated:* It is well known [3], [16] that with an increase in the number of objectives, an increasingly larger fraction of a randomly generated population becomes nondominated. Since most EMO algorithms emphasize nondominated solutions in a population, in handling many-objective problems there is not much room for creating new solutions in a generation. This slows down the search process, and therefore, the overall EMO algorithm becomes inefficient.
- 2) *Evaluation of diversity measure becomes computationally expensive:* To determine the extent of crowding of

solutions in a population, the identification of neighbors becomes computationally expensive in a large-dimensional space. Any compromise or approximation in diversity estimate to make the computations faster may cause an unacceptable distribution of solutions at the end.

- 3) *Recombination operation may be inefficient:* In a many-objective problem, if only a handful of solutions are to be found in a large-dimensional space, solutions are likely to be widely distant from each other. In such a population, the effect of recombination operator (which is considered a key search operator in an EMO) becomes questionable. Two distant parent solutions are likely to produce offspring solutions that are also distant from parents. Thus, special recombination operators (mating restriction or other schemes) may be necessary for handling many-objective problems efficiently.
- 4) *Representation of trade-off surface is difficult:* It is intuitive to realize that to represent a higher dimensional trade-off surface, exponentially more points are needed. Thus, a large population size is needed to represent the resulting Pareto-optimal front. This causes difficulty for a decision-maker to comprehend and make an adequate decision to choose a preferred solution.
- 5) *Performance metrics are computationally expensive to compute:* Since higher-dimensional sets of points are to be compared against each other to establish the performance of one algorithm against another, a larger computational effort is needed. For example, computing hyper-volume metric requires exponentially more computations with the number of objectives [18], [19].
- 6) *Visualization is difficult:* Finally, although it is not a matter related to optimization directly, eventually visualization of a higher-dimensional trade-off front may be difficult for many-objective problems.

The first three difficulties can only be alleviated by certain modifications to existing EMO methodologies. The fourth, fifth, and sixth difficulties are common to all many-objective optimization problems and we do not address them adequately here.

B. EMO Methodologies for Handling Many-Objective Problems

Before we discuss the possible remedies for the three difficulties mentioned above, here we highlight two different many-objective problem classes for which existing EMO methodologies can still be used.

First, existing EMO algorithms may still be useful in finding a preferred subset of solutions (a partial set) from the complete Pareto-optimal set. Although the preferred subset will still be many-dimensional, since the targeted solutions are focused in a small region on the Pareto-optimal front, most of the above difficulties will be alleviated by this principle. A number of MCDM-based EMO methodologies are already devised for this purpose and results in as large as ten-objective problems have shown to perform well [20]–[23].

Second, many problems in practice, albeit having many objectives, often degenerate to result in a low-dimensional

Pareto-optimal front [4], [11], [24], [25]. In such problems, identification of redundant objectives can be integrated with an EMO to find the Pareto-optimal front that is low-dimensional. If the ultimate front is as low as 2-D or 3-D, existing EMO methodologies should work well in handling such problems. A previous study of NSGA-II with a principal component analysis based procedure [4] was able to solve as large as 50-objective problems with a two-objective Pareto-optimal front.

C. Two Ideas for a Many-Objective EMO

Keeping in mind the first three difficulties associated with a domination-based EMO procedure, two different strategies can be considered to alleviate the difficulties.

- 1) *Use of a special domination principle:* The first difficulty mentioned above can be alleviated by using a special domination principle that will adaptively discretize the Pareto-optimal front and find a well-distributed set of points. For example, the use of ϵ -domination principle [26], [27] will make all points within ϵ distance from a set of Pareto-optimal points ϵ -dominated and, hence, the process will generate a finite number of Pareto-optimal points as the target. Such a consideration will also alleviate the second difficulty of diversity preservation. The third difficulty can be taken care of by using a mating restriction scheme or a special recombination scheme in which near-parent solutions are emphasized (such as SBX with a large distribution index [28]). Other special domination principles [29], [30] can also be used for this purpose. Aguirre and Tanaka [31] and Sato *et al.* [32] suggested the use of a subset of objectives for dominance check and for using a different combination of objectives in every generation. The use of fixed cone-domination [33], [34] or variable cone-domination [35] principles can also be tried. These studies were made in the context of low-dimensional problems and their success in solving many-objective optimization is yet to be established.
- 2) *Use of a predefined multiple targeted search:* It is getting increasingly clear that it is too much to expect from a single population-based optimization algorithm to have convergence of its population near the Pareto-optimal front and simultaneously it is distributed uniformly around the entire front in a large-dimensional problem. One way to handle such many-objective optimization problems would be to aid the diversity maintenance issue by some external means. This principle can directly address the second difficulty mentioned above. Instead of searching the entire search space for Pareto-optimal solutions, multiple predefined targeted searches can be set by an algorithm. Since optimal points are found corresponding to each of the targeted search tasks, the first difficulty of dealing with a large nondominated set is also alleviated. The recombination issue can be addressed by using a mating-restriction scheme in which two solutions from neighboring targets are participated in the recombination operation. Our proposed algorithm (NSGA-III) is based on this principle; thus, we discuss

this aspect in somewhat more detail. We suggest two different ways to implement the predefined multiple targeted search principle.

- a) A set of predefined search directions spanning the entire Pareto-optimal front can be specified beforehand and multiple searches can be performed along each direction. Since the search directions are widely distributed, the obtained optimal points are also likely to be widely distributed on the Pareto-optimal front in most problems. A recently proposed MOEA/D procedure [10] uses this concept.
- b) Instead of multiple search directions, multiple predefined reference points can be specified for this purpose. Thereafter, points corresponding to each reference point can be emphasized to find a set of widely distributed sets of Pareto-optimal points. A few such implementations were proposed recently [14], [36]–[38], and this paper suggests another approach extending the algorithm proposed in the first reference [36].

III. EXISTING MANY-OBJECTIVE OPTIMIZATION ALGORITHMS

Garza-Fabre *et al.* [16] suggested three single-objective measures by using differences in individual objective values between two competing parents and showed that in five-objective to 50-objective DTLZ1, DTLZ3, and DTLZ6 problems the convergence property can get enhanced, compared to a number of existing methods including the usual Pareto-dominance-based EMO approaches. Purshouse and Fleming [39] clearly showed that diversity preservation and achieving convergence near the Pareto-optimal front are two contradictory goals, and usual genetic operators are not adequate to attain both goals simultaneously, particularly for many-objective problems. Another study [40] extends NSGA-II by adding diversity-controlling operators to solve six- to 20-objective DTLZ2 problems. Köppen and Yoshida [41] claimed that the NSGA-II procedure in its originality is not suitable for many-objective optimization problems and suggested a number of metrics that can potentially replace NSGA-II's crowding distance operator for better performance. Based on simulation studies on two-objective to 15-objective DTLZ2, DTLZ3, and DTLZ6 problems, they suggested using a substitute assignment distance measure as the best strategy. Hadka and Reed [42] suggested an ensemble-based EMO procedure that uses a suitable recombination operator adaptively chosen from a set of eight to ten different predefined operators based on their generation-wise success rate in a problem. It also uses ϵ -dominance concept and an adaptive population sizing approach that is reported to solve up to eight-objective test problems successfully. Bader and Zitzler [43] suggested a fast procedure for computing sample-based hyper-volume and devised an algorithm to find a set of trade-off solutions for maximizing the hyper-volume. A growing literature on approximate hyper-volume computation [18], [44], [45] may

make such an approach practical for solving many-objective problems.

The above studies analyze and extend previously suggested evolutionary multiobjective optimization algorithms for their suitability to solving many-objective problems. In most cases, the results are promising and the suggested algorithms must be tested on other more challenging problems than the usual normalized test problems such as DTLZ problems. They must also be tried on real-world problems. In the following paragraphs, we describe a recently proposed algorithm that fits well with our description of a many-objective optimization algorithm given in Section II-C and closely matches with our proposed algorithm.

MOEA/D [10] uses a predefined set of weight vectors to maintain a diverse set of trade-off solutions. For each weight vector, the resulting problem is called a subproblem. To start, every population member (with size same as the number of weight vectors) is associated with a weight vector randomly. Thereafter, two solutions from neighboring weight vectors [defined through a niching parameter (T)] are mated and an offspring solution is created. The offspring is then associated with one or more weight vectors based on a performance metric. Two metrics are suggested in the study. A penalized distance measure of a point from the ideal point is formed by weighted sum (weight θ is another algorithmic parameter) of perpendicular distance (d_2) from the reference direction and distance (d_1) along the reference direction

$$\text{PBI}(\mathbf{x}, \mathbf{w}) = d_1 + \theta d_2. \quad (1)$$

Here we call this procedure MOEA/D-PBI. The second approach suggested is the use of Tchebycheff metric using a utopian point \mathbf{z}^* and the weight vector \mathbf{w}

$$\text{TCH}(\mathbf{x}, \mathbf{w}, \mathbf{z}^*) = \max_{i=1}^M w_i |f_i(\mathbf{x}) - z_i^*|. \quad (2)$$

In reported simulations [10], the ideal point was used as \mathbf{z}^* and the zero-weight scenario is handled by using a small number. Here we call this procedure MOEA/D-TCH. An external population maintains the nondominated solutions. The first two difficulties mentioned earlier are negotiated by using an explicit set of weight vectors to find points and the third difficulty is alleviated by using a mating restriction scheme. Simulation results were shown for two-objective and three-objective test problems only, and it was concluded that MOEA/D-PBI is better for three-objective problems than MOEA/D-TCH and the performance of MOEA/D-TCH improved with an objective normalization process using population minimum and maximum objective values. Both versions of MOEA/D require setting a niching parameter (T). Based on some simulation results on two-objective and three-objective problems, the authors suggested the use of a large fraction of population size as T . In addition, MOEA/D-PBI requires an appropriate setting of an additional parameter–penalty parameter θ , for which the authors have suggested a value of 5.

A later study by the developers of MOEA/D suggested the use of differential evolution (DE) to replace genetic recombination and mutation operators. Also, further modifications were done in defining the neighborhood of a particular

solution and in replacing parents in a given neighborhood by the corresponding offspring solutions [46]. Here we call this method MOEA/D-DE. Results on a set of mostly two-objective and three-objective linked problems [47] showed better performance with MOEA/D-DE, compared to other algorithms. As mentioned, MOEA/D is a promising approach for many-objective optimization as it addresses some of the difficulties mentioned above well, but the above-mentioned MOEA/D studies did not quite explore their suitability to a large number of objectives. In this paper, we apply them to problems having up to 15 objectives and evaluate their applicability to truly many-objective optimization problems and reveal interesting properties of these algorithms.

Another recent study [14] follows our description of a many-objective optimization procedure. The study extends the NSGA-II procedure to suggest a hybrid NSGA-II (HN algorithm) for handling three-objective and four-objective problems. Combined population members are projected on a hyperplane and a clustering operation is performed on the hyperplane to select a desired number of clusters, which is user-defined. Thereafter, based on the diversity of the population, either a local search operation on a random cluster member is used to move the solution closer to the Pareto-optimal front, or a diversity enhancement operator is used to choose population members from all clusters. Since no targeted and distributed search is used, the approach is more generic than MOEA/D or the procedure suggested in this paper. However, the efficiency of HN algorithm for problems with more than four objectives is yet to be investigated to suggest its use for many-objective problems in general. We now describe our proposed algorithm.

IV. PROPOSED ALGORITHM: NSGA-III

The basic framework of the proposed many-objective NSGA-II (or NSGA-III) is similar to the original NSGA-II algorithm [5] with significant changes in its selection operator. But, unlike in NSGA-II, the maintenance of diversity among population members in NSGA-III is aided by supplying and adaptively updating a number of well-spread reference points. For completeness, we first present a brief description of the original NSGA-II algorithm.

Let us consider t th generation of NSGA-II algorithm. Suppose the parent population at this generation is P_t and its size is N , while the offspring population created from P_t is Q_t having N members. The first step is to choose the best N members from the combined parent and offspring population $R_t = P_t \cup Q_t$ (of size $2N$), thus allowing us to preserve elite members of the parent population. To achieve this, first the combined population R_t is sorted according to different nondomination levels (F_1, F_2 , and so on). Then, each nondomination level is selected one at a time to construct a new population S_t , starting from F_1 , until the size of S_t is equal to N or for the first time exceeds N . Let us say the last level included is the l th level. Thus, all solutions from level $(l+1)$ onward are rejected from the combined population R_t . In most situations, the last accepted level (l th level) is only accepted partially. In such a case, only those solutions that will maximize the diversity of the l th front are chosen. In

NSGA-II, this is achieved through a computationally efficient, yet approximate, niche-preservation operator that computes the crowding distance for every last level member as the summation of objective-wise normalized distance between two neighboring solutions. Thereafter, the solutions that have larger crowding distance values are chosen. In NSGA-III, we replace the crowding distance operator with the following approaches (Sections IV-A–IV-E).

A. Classification of Population Into Nondominated Levels

The above procedure of identifying nondominated fronts using the usual domination principle [17] is also used in NSGA-III. All population members from the nondominated front level 1 to level l are first included in S_t . If $|S_t| = N$; no further operations are needed and the next generation is started with $P_{t+1} = S_t$. For $|S_t| > N$, members from one to $(l - 1)$ fronts are already selected, i.e., $P_{t+1} = \bigcup_{i=1}^{l-1} F_i$, and the remaining ($K = N - |P_{t+1}|$) population members are chosen from the last front F_l . We describe the remaining selection process in the following subsections.

B. Determination of Reference Points on a Hyper-Plane

As indicated before, NSGA-III uses a predefined set of reference points to ensure diversity in obtained solutions. The chosen reference points can either be predefined in a structured manner or supplied preferentially by the user. We will present results of both methods in the results section later. In the absence of any preference information, any predefined structured placement of reference points can be adopted, but, in this paper, we use Das and Dennis's [48] systematic approach¹ that places points on a normalized hyper-plane—an $(M - 1)$ -dimensional unit simplex—which is equally inclined to all objective axes and has an intercept of one on each axis. If p divisions are considered along each objective, the total number of reference points (H) in an M -objective problem is given by

$$H = \binom{M + p - 1}{p}. \quad (3)$$

For example, in a three-objective problem ($M = 3$), the reference points are created on a triangle with the apex at $(1, 0, 0)$, $(0, 1, 0)$, and $(0, 0, 1)$. If four divisions ($p = 4$) are chosen for each objective axis $H = \binom{3+4-1}{4}$ or 15 reference points will be created. For clarity, these reference points are shown in Fig. 1. In the proposed NSGA-III, in addition to emphasizing nondominated solutions, we also emphasize population members that are in some sense associated with each of these reference points. Since the above-created reference points are widely distributed on the entire normalized hyperplane, the obtained solutions are also likely to be widely distributed on or near the Pareto-optimal front. In the case of a user-supplied set of preferred reference points, ideally the user can mark H points on the normalized hyper-plane or indicate any H , M -dimensional vectors for the purpose. The proposed algorithm is likely to find near Pareto-optimal solutions corresponding to the supplied reference points, thereby allowing

¹Any other structured distribution with or without a biasing on some part of the Pareto-optimal front can be used as well.

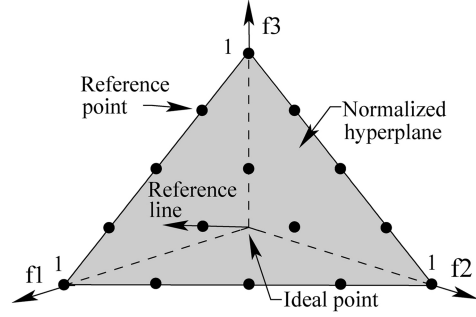


Fig. 1. Fifteen structured reference points are shown on a normalized reference plane for a three-objective problem with $p = 4$.

Algorithm 1 Generation t of NSGA-III procedure

Input: H structured reference points Z^s or supplied aspiration points Z^a , parent population P_t

Output: P_{t+1}

- 1: $S_t = \emptyset$, $i = 1$
- 2: $Q_t = \text{Recombination+Mutation}(P_t)$
- 3: $R_t = P_t \cup Q_t$
- 4: $(F_1, F_2, \dots) = \text{Non-dominated-sort}(R_t)$
- 5: **repeat**
- 6: $S_t = S_t \cup F_i$ and $i = i + 1$
- 7: **until** $|S_t| \geq N$
- 8: Last front to be included: $F_l = F_i$
- 9: **if** $|S_t| = N$ **then**
- 10: $P_{t+1} = S_t$, break
- 11: **else**
- 12: $P_{t+1} = \bigcup_{j=1}^{l-1} F_j$
- 13: Points to be chosen from F_l : $K = N - |P_{t+1}|$
- 14: Normalize objectives and create reference set Z^r : $\text{Normalize}(\mathbf{f}^n, S_t, Z^r, Z^s, Z^a)$
- 15: Associate each member s of S_t with a reference point: $[\pi(s), d(s)] = \text{Associate}(S_t, Z^r)$ % $\pi(s)$: closest reference point, d : distance between s and $\pi(s)$
- 16: Compute niche count of reference point $j \in Z^r$: $\rho_j = \sum_{s \in S_t / F_l} (\pi(s) = j) ? 1 : 0$
- 17: Choose K members one at a time from F_l to construct P_{t+1} : $\text{Niching}(K, \rho_j, \pi, d, Z^r, F_l, P_{t+1})$
- 18: **end if**

this method to be used more from the point of view of a combined application of decision-making and many-objective optimization. The procedure is presented in Algorithm 1.

C. Adaptive Normalization of Population Members

First, the ideal point of the population S_t is determined by identifying the minimum value (z_i^{\min}) for each objective function $i = 1, 2, \dots, M$ in $\bigcup_{\tau=0}^t S_\tau$ and by constructing the ideal point $\bar{z} = (z_1^{\min}, z_2^{\min}, \dots, z_M^{\min})$. Each objective value of S_t is then translated by subtracting objective f_i by z_i^{\min} so that the ideal point of translated S_t becomes a zero vector. We denote this translated objective as $f'_i(\mathbf{x}) = f_i(\mathbf{x}) - z_i^{\min}$. Thereafter, the extreme point ($\mathbf{z}^{i,\max}$) in each (i th) objective axis is identified by finding the solution ($\mathbf{x} \in S_t$) that makes the corresponding achievement scalarizing function (formed with $f'_i(\mathbf{x})$ and a weight vector close to i th objective axis) minimum.

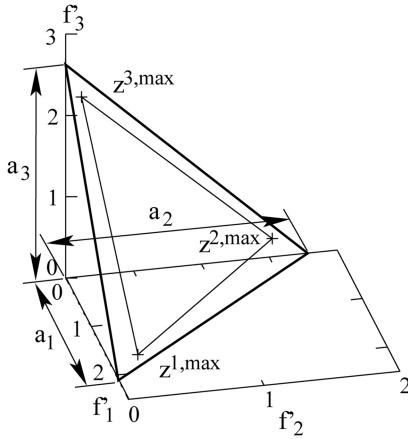


Fig. 2. Procedure for computing intercepts and then forming the hyper-plane from extreme points are shown for a three-objective problem.

These M extreme vectors are then used to constitute an M -dimensional hyper-plane. The intercept a_i of the i th objective axis and the linear hyper-plane can then be computed (see Fig. 2). Special care is taken to handle degenerate cases and nonnegative intercepts. The objective functions can then be normalized as

$$f_i^n(\mathbf{x}) = \frac{f'_i(\mathbf{x})}{a_i}, \quad \text{for } i = 1, 2, \dots, M. \quad (4)$$

Note that the intercept on each normalized objective axis is now at $f_i^n = 1$, and a hyper-plane constructed with these intercept points will make $\sum_{i=1}^M f_i^n = 1$.

In the case of structured reference points (H of them), the original reference points calculated using Das and Dennis's [48] approach already lie on this normalized hyper-plane. In the case of preferred reference points by the user, the reference points are simply mapped onto the above-constructed normalized hyper-plane using (4). Since the normalization procedure and the creation of the hyper-plane is done at each generation using extreme points ever found from the start of the simulation, the proposed NSGA-III procedure adaptively maintains a diversity in the space spanned by the members of S_t at every generation. This enables NSGA-III to solve problems with a Pareto-optimal front whose objective values may be differently scaled. The procedure is also described in Algorithm 2.

D. Association Operation

After normalizing each objective adaptively based on the extent of members of S_t in the objective space, we need to associate each population member with a reference point. For this purpose, we define a reference line corresponding to each reference point on the hyper-plane by joining the reference point with the origin. Then, we calculate the perpendicular distance of each population member of S_t from each of the reference lines. The reference point whose reference line is closest to a population member in the normalized objective space is considered to be associated with the population member. This is illustrated in Fig. 3. The procedure is presented in Algorithm 3.

Algorithm 2 Normalize $(\mathbf{f}^n, S_t, Z^r, Z^s/Z^a)$ procedure

Input: S_t , Z^s (structured points) or Z^a (supplied points)
Output: \mathbf{f}^n , Z^r (reference points on normalized hyper-plane)

- 1: **for** $j = 1$ to M **do**
- 2: Compute ideal point: $z_j^{\min} = \min_{\mathbf{s} \in S_t} f_j(\mathbf{s})$
- 3: Translate objectives: $f'_j(\mathbf{s}) = f_j(\mathbf{s}) - z_j^{\min} \quad \forall \mathbf{s} \in S_t$
- 4: Compute extreme points $(\mathbf{z}^{i,\max}, j = 1, \dots, M)$ of S_t
- 5: **end for**
- 6: Compute intercepts a_j for $j = 1, \dots, M$
- 7: Normalize objectives (\mathbf{f}^n) using Equation 4
- 8: **if** Z^a is given **then**
- 9: Map each (aspiration) point on normalized hyper-plane using Equation 4 and save the points in the set Z^r
- 10: **else**
- 11: $Z^r = Z^s$
- 12: **end if**

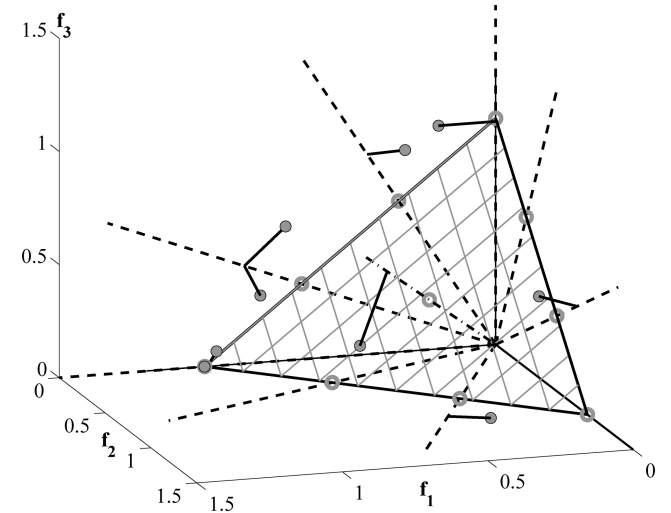


Fig. 3. Association of population members with reference points is illustrated.

Algorithm 3 Associate (S_t, Z^r) procedure

Input: Z^r, S_t
Output: $\pi(\mathbf{s} \in S_t), d(\mathbf{s} \in S_t)$

- 1: **for** each reference point $\mathbf{z} \in Z^r$ **do**
- 2: Compute reference line $\mathbf{w} = \mathbf{z}$
- 3: **end for**
- 4: **for** each $\mathbf{s} \in S_t$ **do**
- 5: **for** each $\mathbf{w} \in Z^r$ **do**
- 6: Compute $d^\perp(\mathbf{s}, \mathbf{w}) = \|(\mathbf{s} - \mathbf{w}^T \mathbf{s} / \|\mathbf{w}\|^2)\|$
- 7: **end for**
- 8: Assign $\pi(\mathbf{s}) = \mathbf{w} : \operatorname{argmin}_{\mathbf{w} \in Z^r} d^\perp(\mathbf{s}, \mathbf{w})$
- 9: Assign $d(\mathbf{s}) = d^\perp(\mathbf{s}, \pi(\mathbf{s}))$
- 10: **end for**

E. Niche-Preservation Operation

It is worth noting that a reference point may have one or more population members associated with it or need not have any population member associated with it. We count the number of population members from $P_{t+1} = S_t/F_t$ that are associated with each reference point. Let us denote this niche

Algorithm 4 Niching ($K, \rho_j, \pi, d, Z^r, F_l, P_{t+1}$) procedure**Input:** $K, \rho_j, \pi(s \in S_t), d(s \in S_t), Z^r, F_l$ **Output:** P_{t+1}

```

1:  $k = 1$ 
2: while  $k \leq K$  do
3:    $J_{\min} = \{j : \operatorname{argmin}_{j \in Z^r} \rho_j\}$ 
4:    $\bar{j} = \text{random}(J_{\min})$ 
5:    $I_{\bar{j}} = \{s : \pi(s) = \bar{j}, s \in F_l\}$ 
6:   if  $I_{\bar{j}} \neq \emptyset$  then
7:     if  $\rho_{\bar{j}} = 0$  then
8:        $P_{t+1} = P_{t+1} \cup \left( s : \operatorname{argmin}_{s \in I_{\bar{j}}} d(s) \right)$ 
9:     else
10:     $P_{t+1} = P_{t+1} \cup \text{random}(I_{\bar{j}})$ 
11:   end if
12:    $\rho_{\bar{j}} = \rho_{\bar{j}} + 1, F_l = F_l \setminus s$ 
13:    $k = k + 1$ 
14: else
15:    $Z^r = Z^r / \{\bar{j}\}$ 
16: end if
17: end while

```

count as ρ_j for the j th reference point. We now devise a new niche-preserving operation as follows. First, we identify the reference point set $J_{\min} = \{j : \operatorname{argmin}_j \rho_j\}$ having minimum ρ_j . In the case of multiple such reference points, one ($\bar{j} \in J_{\min}$) is chosen at random.

If $\rho_{\bar{j}} = 0$ (meaning that there is no associated P_{t+1} member to the reference point \bar{j}), there can be two scenarios with \bar{j} in set F_l . First, there exists one or more members in front F_l that are associated with the reference point \bar{j} . In this case, the one having the shortest perpendicular distance from the reference line is added to P_{t+1} . The count $\rho_{\bar{j}}$ for reference point \bar{j} is then incremented by one. Second, the front F_l does not have any member associated with the reference point \bar{j} . In this case, the reference point is excluded from further consideration for the current generation.

In the event of $\rho_{\bar{j}} \geq 1$ (meaning that already one member associated with the reference point exists in S_t/F_l), a randomly² chosen member, if exists, from front F_l that is associated with the reference point \bar{j} is added to P_{t+1} . The count $\rho_{\bar{j}}$ is then incremented by one. After niche counts are updated, the procedure is repeated for a total of K times (see Section IV-A) to fill all vacant population slots of P_{t+1} . The procedure is presented in Algorithm 4.

F. Genetic Operations to Create Offspring Population

After P_{t+1} is formed, it is then used to create a new offspring population Q_{t+1} by applying usual genetic operators. In NSGA-III, we have already performed a careful elitist selection of solutions and attempted to maintain diversity among solutions by emphasizing solutions closest to the reference line of each reference point. Also, as we will describe in Section V, for a computationally fast procedure, we have set N almost equal to H , thereby expecting to evolve one population

²The point closest to the reference point or using any other diversity preserving criterion can also be used.

member close to the Pareto-optimal front corresponding to each reference point. For all these reasons, we do not employ any explicit reproduction operation with NSGA-III for handling problems with box constraints only. The population Q_{t+1} is constructed by applying the usual crossover and mutation operators by randomly picking parents from P_{t+1} . However, to create offspring solutions closer to parent solutions (to take care of third difficulty mentioned in Section II-A), we suggest using a relatively larger value of distribution index in the SBX operator, thereby creating offsprings close to their parents.

G. Computational Complexity of One Generation of NSGA-III

The nondominated sorting (line 4 in Algorithm 1) of a population of size $2N$ having M -dimensional objective vectors requires $O(N \log^{M-2} N)$ computations [49]. Identification of the ideal point in line 2 of Algorithm 2 requires a total of $O(MN)$ computations. A translation of objectives (line 3) requires $O(MN)$ computations. However, identification of extreme points (line 4) requires $O(M^2 N)$ computations. Determination of intercepts (line 6) requires one matrix inversion of size $M \times M$, requiring $O(M^3)$ operations. Thereafter, normalization of a maximum of $2N$ population members (line 7) requires $O(N)$ computations. Line 8 of Algorithm 2 requires $O(MH)$ computations. All operations in Algorithm 3 in associating a maximum of $2N$ population members to H reference points would require $O(MNH)$ computations. Thereafter, in the niching procedure in Algorithm 4, line 3 will require $O(H)$ comparisons. Assuming that $L = |F_l|$, line 5 requires $O(L)$ checks. Line 8 in the worst case requires $O(L)$ computations. Other operations have smaller complexity. However, the above computations in the niching algorithm need to be performed a maximum of L times, thereby requiring larger of $O(L^2)$ or $O(LH)$ computations. In the worst case scenario ($S_t = F_l$, i.e., the first nondominated front exceeds the population size), $L \leq 2N$. In all of our simulations, we have used $N \approx H$ and usually $N > M$. Taking into account all the above considerations and computations, the overall worst-case complexity of one generation of NSGA-III is $O(N^2 \log^{M-2} N)$ or $O(N^2 M)$, whichever is larger.

H. Parameter-Less Property of NSGA-III

As in NSGA-II, the NSGA-III algorithm does not require setting any new parameter other than the usual GA parameters such as the population size, termination parameter, crossover and mutation probabilities, and their associated parameters. The number of reference points H is not an algorithmic parameter, as this is directly related to the desired number of trade-off points. The population size N is dependent on H , as $N \approx H$. The location of the reference points is similarly dependent on the preference information that the user is interested to achieve in the obtained solutions.

We will now present simulation results of NSGA-III for various many-objective scenarios and compare its performance with MOEA/D and classical methods.

V. RESULTS

In this section, we provide the simulation results of NSGA-III on three-objective to 15-objective optimization

TABLE I

NUMBER OF REFERENCE POINTS/DIRECTIONS AND CORRESPONDING POPULATION SIZES USED IN NSGA-III AND MOEA/D ALGORITHMS

No. of objectives (M)	Ref. pts./Ref. dim. (H)	NSGA-III popsize (N)	MOEA/D popsize (N')
3	91	92	91
5	210	212	210
8	156	156	156
10	275	276	275
15	135	136	135

problems. Since our method has a framework similar to MOEA/D in that both types of algorithms require a set of user-supplied reference points or weight vectors, we compare our proposed method with different versions of MOEA/D (codes from MOEA/D website [50] are used). The original MOEA/D study proposed two procedures (MOEA/D-PBI and MOEA/D-TCH), but did not solve four or more-objective problems. Here, along with our algorithm, we investigate the performance of these MOEA/D algorithms on three-objective to 15-objective problems.

As a performance metric, we have chosen the inverse generational distance (IGD) metric [47], [51], which as a single metric can provide a combined information about the convergence and diversity of the obtained solutions. Since reference points or reference directions are supplied in NSGA-III and MOEA/D algorithms, respectively, and since in this section we show the working of these methods on test problems for which the exact Pareto-optimal surface is known, we can exactly locate the targeted Pareto-optimal points by finding the intersection point of the Pareto-optimal surface with each reference line. We compute these targeted points (\mathbf{z}_i) and call them a set \mathbf{Z}_{eff} . For any algorithm, we obtain the final nondominated points in the objective space and call them the set \mathbf{A} . Now, we compute the IGD metric as the average Euclidean distance of points in set \mathbf{Z}_{eff} with their nearest members of all points in set \mathbf{A} as

$$\text{IGD}(\mathbf{A}, \mathbf{Z}_{\text{eff}}) = \frac{1}{|\mathbf{Z}_{\text{eff}}|} \sum_{i=1}^{|\mathbf{Z}_{\text{eff}}|} \min_{j=1}^{|\mathbf{A}|} d(\mathbf{z}_i, \mathbf{a}_j) \quad (5)$$

where $d(\mathbf{z}_i, \mathbf{a}_j) = \|\mathbf{z}_i - \mathbf{a}_j\|_2$. It is not necessary to write that a set with a smaller IGD value is better. If no solution associated with a reference point is found, the IGD metric value for the set will be large. For each case, 20 different runs from different initial populations are performed, and best, median, and worst IGD performance values are reported. For all algorithms, the population members from the final generation are presented and used for computing the performance measure.

Table I shows the number of chosen reference points (H) for different sizes of a problem. The population size N for NSGA-III is set as the smallest multiple of four³ larger than H . For MOEA/D procedures, we use a population size, $N' = H$, as suggested by their developers. For three-objective problems, we have used $p = 12$ in order to obtain $H = \binom{3-1+12}{12}$ or 91

³Since no tournament selection is used in NSGA-III, a factor of two would be adequate as well, but as we reintroduce tournament selection in the constrained NSGA-III in the sequel paper [52], we keep population size as a multiple of four here as well to have a unified algorithm.

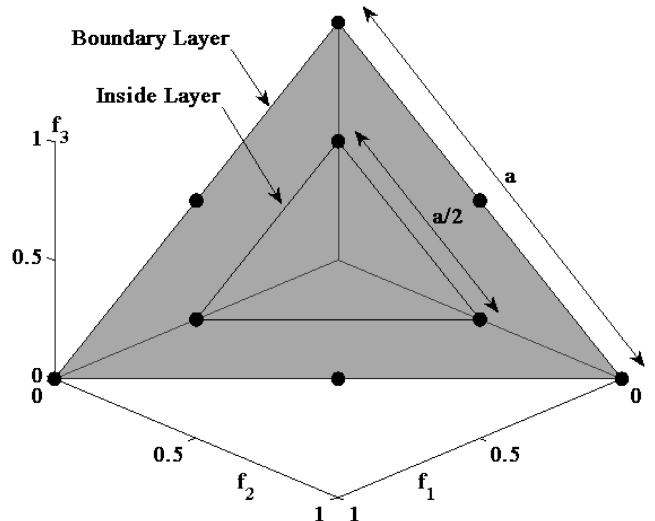


Fig. 4. Concept for two-layered reference points [with six points on the boundary layer ($p = 2$) and three points on the inside layer ($p = 1$)] is shown for a three-objective problem, but is implemented for eight or more objectives in the simulations here.

TABLE II
PARAMETER VALUES USED IN NSGA-III AND TWO VERSIONS OF MOEA/D. n IS THE NUMBER OF VARIABLES

Parameters	NSGA-III	MOEA/D
SBX probability [28], p_c	1	1
Polynomial mutation prob. [3], p_m	$1/n$	$1/n$
η_c [28]	30	20
η_m [28]	20	20

reference points [refer to (3)]. For five-objective problems, we have used $p = 6$ so that $H = 210$ reference points are obtained. Note that as long as $p \geq M$ is not chosen, no intermediate point will be created by Das and Dennis's systematic approach. For eight-objective problems, even if we use $p = 8$ (to have exactly one intermediate reference point), it requires 5040 reference points. To avoid such a situation, we use two layers of reference points with relatively small values of p . On the boundary layer, we use $p = 3$ so that 120 points are created. On the inside layer, we use $p = 2$ so that 36 points are created. All $H = 156$ points are then used as reference points for eight-objective problems. We illustrate this scenario in Fig. 4 for a three-objective problem using $p = 2$ for the boundary layer and $p = 1$ for the inside layer.

For ten-objective problems as well, we use $p = 3$ and $p = 2$ for boundary and inside layers, respectively, thereby requiring a total of $H = 220 + 55$ or 275 reference points. Similarly, for 15-objective problems, we use $p = 2$ and $p = 1$ for boundary and inside layers, respectively, thereby requiring $H = 120 + 15$ or 135 reference points.

Table II presents other NSGA-III and MOEA/D parameters used in this paper. MOEA/D requires additional parameters that we have set according to the suggestions given by their developers. The neighborhood size T is set as 20 for both approaches and, additionally, the penalty parameter θ for the MOEA/D-PBI approach is set as 5.

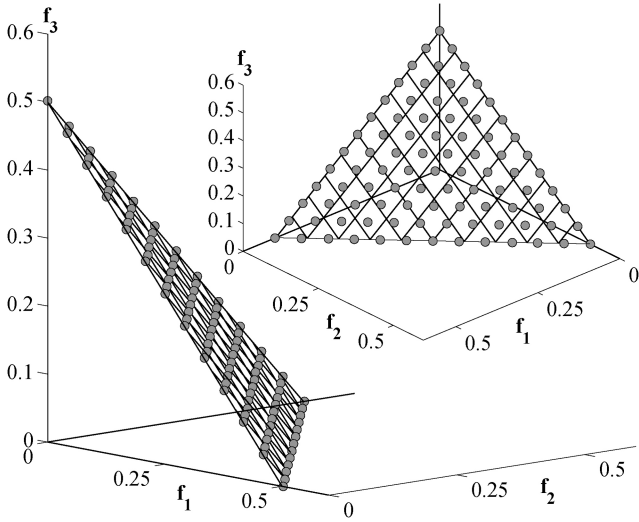


Fig. 5. Obtained solutions by NSGA-III for DTLZ1.

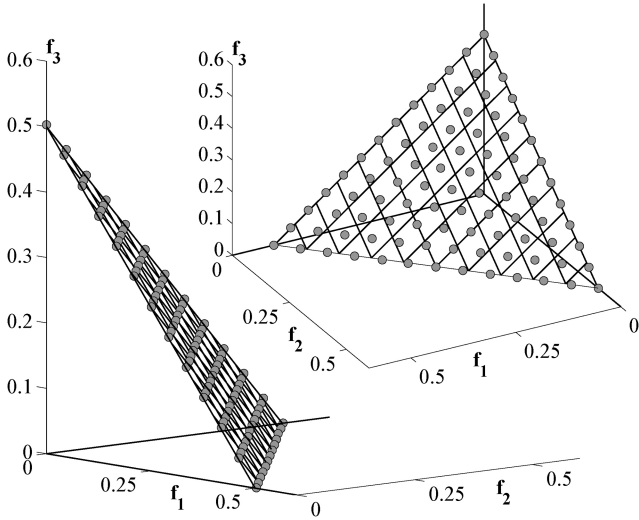


Fig. 6. Obtained solutions by MOEA/D-PBI for DTLZ1.

A. Normalized Test Problems

To start, we use 3- to 15-objective DTLZ1, DTLZ2, DTLZ3, and DTLZ4 problems [53]. The number of variables are $(M + k - 1)$, where M is the number of objectives and $k = 5$ for DTLZ1, while $k = 10$ for DTLZ2, DTLZ3, and DTLZ4. The corresponding Pareto-optimal fronts lie in $f_i \in [0, 0.5]$ for the DTLZ1 problem and in $f_i \in [0, 1]$ for other DTLZ problems. Since they have an identical range of values for each objective, we call these problems normalized test problems in this paper. Table III indicates the maximum number of generations used for each test problem.

Fig. 5 shows NSGA-III obtained front for the three-objective DTLZ1 problem. This particular run is associated with the median value of IGD performance metric. All 91 points are well distributed on the entire Pareto-optimal set. Results with the MOEA/D-PBI are shown in Fig. 6. It is clear that MOEA/D-PBI is also able to find a good distribution of points similar to that of NSGA-III. However, Fig. 7 shows that MOEA/D-TCH is unable to find a uniform distribution of

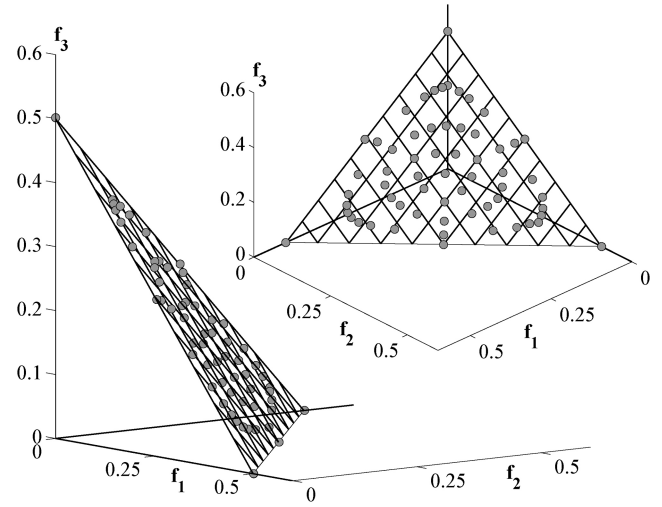


Fig. 7. Obtained solutions by MOEA/D-TCH for DTLZ1.

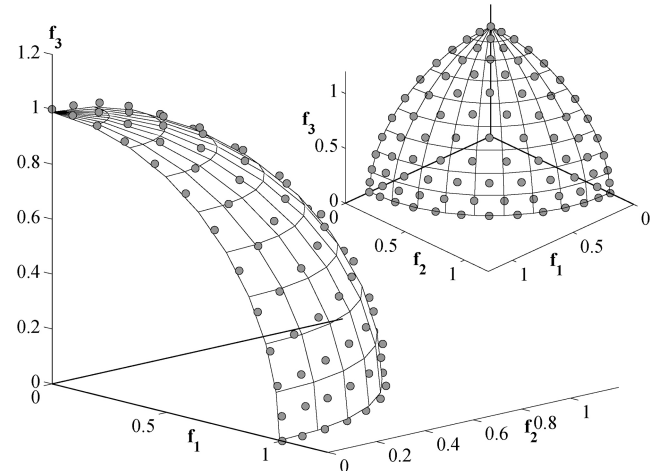


Fig. 8. Obtained solutions by NSGA-III for DTLZ2.

points. Such a distribution was also reported in the original MOEA/D study [10].

Table III shows that for the DTLZ1 problem NSGA-III performs slightly better in terms of the IGD metric, followed by MOEA/D-PBI. For the five-objective DTLZ1 problem, MOEA/D performs better than NSGA-III, but in 8-, 10-, and 15-objective problems, NSGA-III performs better. MOEA/D-TCH consistently does not perform well in all higher dimensional versions of the problem. This observation is similar to that concluded in the original MOEA/D study [10] based on two-objective and three-objective problems.

For DTLZ2 problems, the performance of MOEA/D-PBI is consistently better than NSGA-III; however, NSGA-III performs better than the MOEA/D-TCH approach. Figs. 8–10 show the distribution of obtained points for NSGA-III, MOEA/D-PBI, and MOEA/D-TCH algorithms on the three-objective DTLZ2 problem, respectively. The figures show that the performances of NSGA-III and MOEA/D-PBI are comparable to each other, whereas the performance of MOEA/D-TCH is poor.

TABLE III

BEST, MEDIAN, AND WORST IGD VALUES OBTAINED FOR NSGA-III AND TWO VERSIONS OF MOEA/D ON M -OBJECTIVE DTLZ1, DTLZ2, DTLZ3, AND DTLZ4 PROBLEMS. BEST PERFORMANCE IS SHOWN IN BOLD

Problem	M	MaxGen	NSGA-III	MOEA/D-PBI	MOEA/D-TCH	MOEA/D-DE
DTLZ1	3	400	4.880×10^{-4}	4.095×10^{-4}	3.296×10^{-2}	5.470×10^{-3}
			1.308×10^{-3}	1.495×10^{-3}	3.321×10^{-2}	1.778×10^{-2}
			4.880×10^{-3}	4.743×10^{-3}	3.359×10^{-2}	3.394×10^{-1}
	5	600	5.116×10^{-4}	3.179×10^{-4}	1.124×10^{-1}	2.149×10^{-2}
			9.799×10^{-4}	6.372×10^{-4}	1.129×10^{-1}	2.489×10^{-2}
			1.979×10^{-3}	1.635×10^{-3}	1.137×10^{-1}	3.432×10^{-2}
DTLZ2	8	750	2.044×10^{-3}	3.914×10^{-3}	1.729×10^{-1}	3.849×10^{-2}
			3.979×10^{-3}	6.106×10^{-3}	1.953×10^{-1}	4.145×10^{-2}
			8.721×10^{-3}	8.537×10^{-3}	2.094×10^{-1}	4.815×10^{-2}
	10	1000	2.215×10^{-3}	3.872×10^{-3}	2.072×10^{-1}	4.253×10^{-2}
			3.462×10^{-3}	5.073×10^{-3}	2.147×10^{-1}	4.648×10^{-2}
			6.869×10^{-3}	6.130×10^{-3}	2.400×10^{-1}	4.908×10^{-2}
DTLZ3	15	1500	2.649×10^{-3}	1.236×10^{-2}	3.237×10^{-1}	8.048×10^{-2}
			5.063×10^{-3}	1.431×10^{-2}	3.438×10^{-1}	8.745×10^{-2}
			1.123×10^{-2}	1.692×10^{-2}	3.634×10^{-1}	1.008×10^{-1}
	3	250	1.262×10^{-3}	5.432×10^{-4}	7.499×10^{-2}	3.849×10^{-2}
			1.357×10^{-3}	6.406×10^{-4}	7.574×10^{-2}	4.562×10^{-2}
			2.114×10^{-3}	8.006×10^{-4}	7.657×10^{-2}	6.069×10^{-2}
DTLZ4	5	350	4.254×10^{-3}	1.219×10^{-3}	2.935×10^{-1}	1.595×10^{-1}
			4.982×10^{-3}	1.437×10^{-3}	2.945×10^{-1}	1.820×10^{-1}
			5.862×10^{-3}	1.727×10^{-3}	2.953×10^{-1}	1.935×10^{-1}
	8	500	1.371×10^{-2}	3.097×10^{-3}	5.989×10^{-1}	3.003×10^{-1}
			1.571×10^{-2}	3.763×10^{-3}	6.301×10^{-1}	3.194×10^{-1}
			1.811×10^{-2}	5.198×10^{-3}	6.606×10^{-1}	3.481×10^{-1}
DTLZ4	10	750	1.350×10^{-2}	2.474×10^{-3}	7.002×10^{-1}	2.629×10^{-1}
			1.528×10^{-2}	2.778×10^{-3}	7.266×10^{-1}	2.873×10^{-1}
			1.697×10^{-2}	3.235×10^{-3}	7.704×10^{-1}	3.337×10^{-1}
	15	1000	1.360×10^{-2}	5.254×10^{-3}	1.000	3.131×10^{-1}
			1.726×10^{-2}	6.005×10^{-3}	1.084	3.770×10^{-1}
			2.114×10^{-2}	9.409×10^{-3}	1.120	4.908×10^{-1}

Fig. 11 shows the variation of the IGD metric value with function evaluations for NSGA-III and MOEA/D-PBI approaches for the eight-objective DTLZ2 problem. Average IGD metric values for 20 runs are plotted. It is clear that both approaches are able to reduce the IGD value with an elapse of function evaluations.

A similar observation is made for the DTLZ3 problem. This problem introduces a number of local Pareto-optimal fronts that provide a stiff challenge for algorithms to come close to the global Pareto-optimal front. While the performances of NSGA-III and MOEA/D-PBI are similar, with a slight edge for MOEA/D-PBI, the performance of MOEA/D-TCH is poor.

However, in some runs, MOEA/D-PBI is unable to get close to the Pareto-optimal front, as evident from a large value of IGD metric value. Fig. 12 shows variation of the average IGD metric of 20 runs with function evaluations for NSGA-III and MOEA/D-PBI approaches. NSGA-III manages to find a better IGD value than the MOEA/D-PBI approach after about 80 000 function evaluations.

Problem DTLZ4 has a biased density of points away from $f_M = 0$; however, the Pareto-optimal front is identical to that in DTLZ2. The difference in the performances between NSGA-III and MOEA/D-PBI is clear from this problem. Both MOEA/D algorithms are not able to find an adequate distribu-

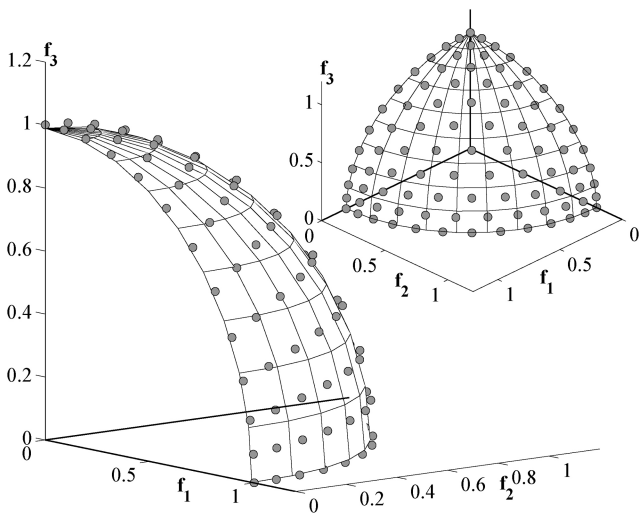


Fig. 9. Obtained solutions by MOEA/D-PBI for DTLZ2.

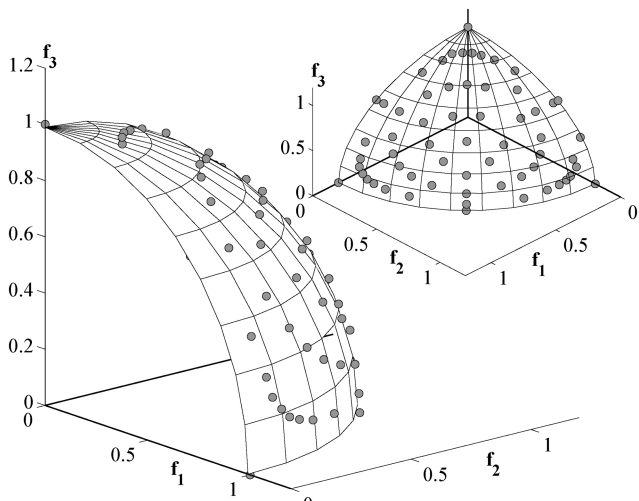


Fig. 10. Obtained solutions by MOEA/D-TCH for DTLZ2.

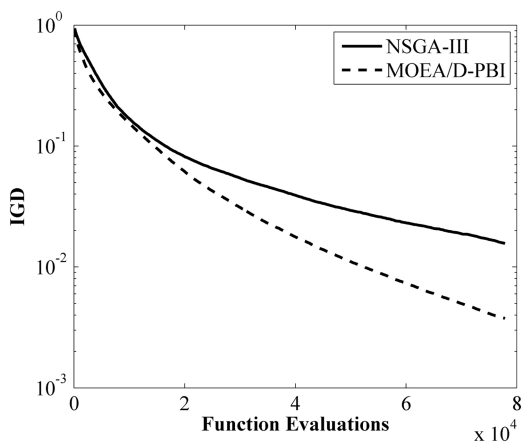


Fig. 11. Variation of IGD metric value with NSGA-III and MOEA/D-PBI for DTLZ2.

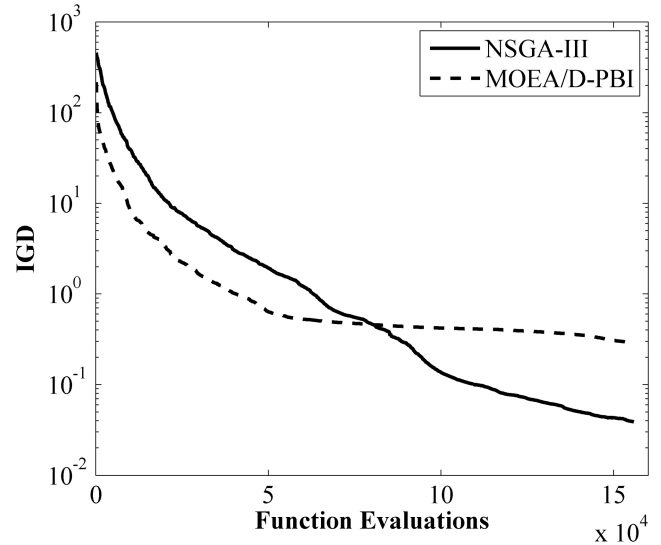


Fig. 12. Variation of IGD metric value with NSGA-III and MOEA/D-PBI for DTLZ3.

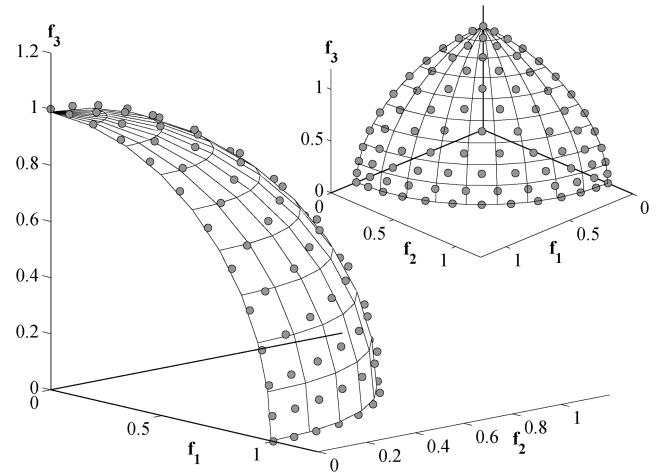


Fig. 13. Obtained solutions by NSGA-III for DTLZ4.

tion of points, whereas the NSGA-III algorithm performs as it did in other problems. Figs. 13–15 show the obtained distribution of points on the three-objective DTLZ4 problem. The algorithms are unable to find near $f_3 = 0$ Pareto-optimal points, whereas the NSGA-III is able to find a set of well-distributed points on the entire Pareto-optimal front. These plots are made using the median performed run in each case. Table III clearly shows that the IGD metric values for NSGA-III algorithm are better than those of MOEA/D algorithms. Fig. 16 shows the value path plot of all obtained solutions for the ten-objective DTLZ4 problem by NSGA-III. A spread of solutions over $f_i \in [0, 1]$ for all ten objectives and a trade-off among them are clear from the plot. In contrast, Fig. 17 shows the value path plot for the same problem obtained using MOEA/D-PBI. The figure clearly shows that MOEA/D-PBI is not able to find a widely distributed set of points for the ten-objective DTLZ4 problem. Points having larger values of objectives f_1 to f_7 are not found by the MOEA/D-PBI approach.

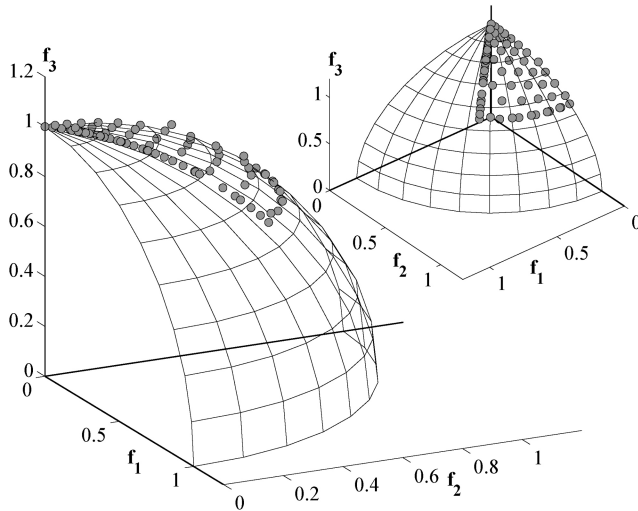


Fig. 14. Obtained solutions by MOEA/D-PBI for DTLZ4.

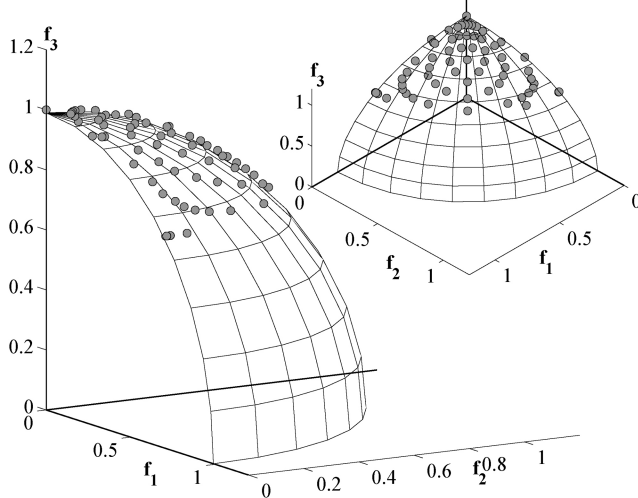


Fig. 15. Obtained solutions by MOEA/D-TCH for DTLZ4.

The right-most column of Table III presents the performance of the recently proposed MOEA/D-DE approach [46]. The approach uses differential evolution (DE) instead of SBX and polynomial mutation operators. Two additional parameters are introduced in the MOEA/D-DE procedure. First, a maximum bound (n_r) on the number of weight vectors with which a child can be associated is introduced and is set as $n_r = 2$. Second, for choosing a mating partner of a parent, a probability (δ) is set for choosing a neighboring partner and the probability $(1 - \delta)$ for choosing any other population member. Authors suggested using $\delta = 0.9$. We use the same values of these parameters in our study. Table III indicates that this version of MOEA/D does not perform well on the normalized DTLZ problems; however, it performs better than MOEA/D-PBI on the DTLZ4 problem. Due to its poor performance in these problems in general, we do not apply it any further.

In the above runs with MOEA/D, we have used the SBX recombination parameter index $\eta_c = 20$ (as indicated in Table II) mainly because this value was chosen in the original MOEA/D study [10]. Next, we investigate MOEA/D-PBIs

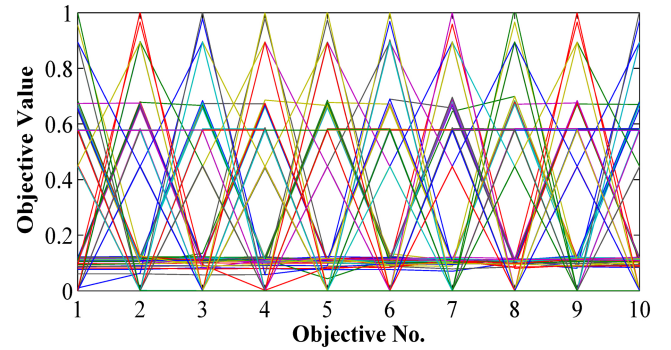


Fig. 16. NSGA-III solutions are shown using ten-objective value path format for DTLZ4.

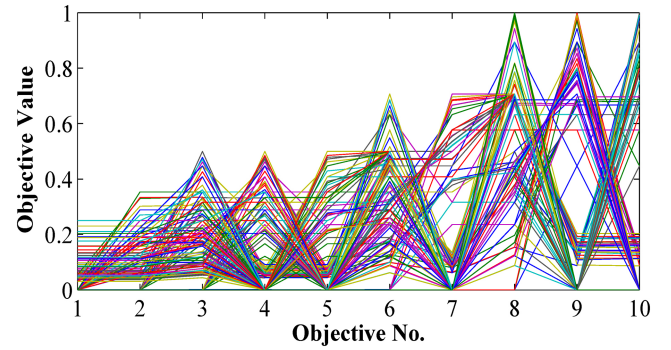


Fig. 17. MOEA/D-PBI solutions are shown using ten-objective value path format for DTLZ4.

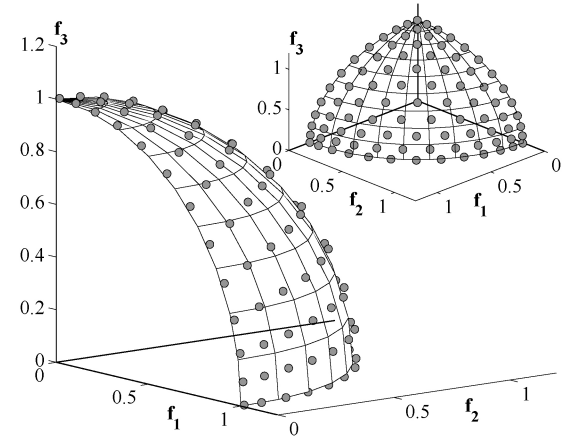


Fig. 18. NSGA-III solutions on the three-objective WFG6 problem.

performance with $\eta_c = 30$ (which was used with NSGA-III). Table IV shows that the performance of MOEA/D does not change much with the above change in the η_c value.

Next, we apply NSGA-III and MOEA/D-PBI approaches to two WFG test problems. The parameter settings are the same as before. Figs. 18 and 19 show the obtained points on the WFG6 problem. The convergence is slightly better with the NSGA-III approach. Similarly, Figs. 20 and 21 show a similar performance comparison of the above two approaches for the WFG7 problem. Table V shows the performances of the two approaches up to 15-objective WFG6 and WFG7 problems.

TABLE IV
IGD VALUES OF MOEA/D-PBI APPROACH WITH $\eta_c = 30$.

Function	M	MaxGen	NSGA-III	MOEA/D-PBI
DTLZ1	3	400	4.880×10^{-4}	4.047×10^{-4}
			1.308×10^{-3}	1.797×10^{-3}
			4.880×10^{-3}	5.699×10^{-3}
	5	600	5.116×10^{-4}	2.849×10^{-4}
			9.799×10^{-4}	5.717×10^{-4}
DTLZ2	8	750	2.044×10^{-3}	4.053×10^{-3}
			3.979×10^{-3}	6.839×10^{-3}
			8.721×10^{-3}	1.127×10^{-2}
	10	1000	2.215×10^{-3}	4.057×10^{-3}
			3.462×10^{-3}	5.251×10^{-3}
DTLZ3	15	1500	6.869×10^{-3}	6.300×10^{-3}
			2.649×10^{-3}	1.301×10^{-2}
			5.063×10^{-3}	1.653×10^{-2}
			1.123×10^{-2}	2.695×10^{-2}
DTLZ4	3	600	2.915×10^{-4}	1.092×10^{-1}
			5.970×10^{-4}	4.277×10^{-1}
			4.286×10^{-1}	5.235×10^{-1}
	5	1000	9.849×10^{-4}	2.342×10^{-1}
			1.255×10^{-3}	4.384×10^{-1}
DTLZ5	8	1250	1.721×10^{-3}	7.347×10^{-1}
			5.079×10^{-3}	3.821×10^{-1}
			7.054×10^{-3}	8.015×10^{-1}
			6.051×10^{-1}	9.686×10^{-1}
DTLZ6	10	2000	5.694×10^{-3}	5.083×10^{-1}
			6.337×10^{-3}	8.321×10^{-1}
			1.076×10^{-1}	1.024
	15	3000	7.110×10^{-3}	9.406×10^{-1}
			3.431×10^{-1}	1.157
			1.073	1.219

Based on the results on three- to 15-objective normalized DTLZ and WFG test problems, it can be concluded that: 1) MOEA/D-PBI performs consistently better than MOEA/D-TCH approach; 2) MOEA/D-PBI performs best in some problems, whereas the proposed NSGA-III approach performs best in some other problems; and 3) in a nonuniformly distributed Pareto-optimal front (as in the

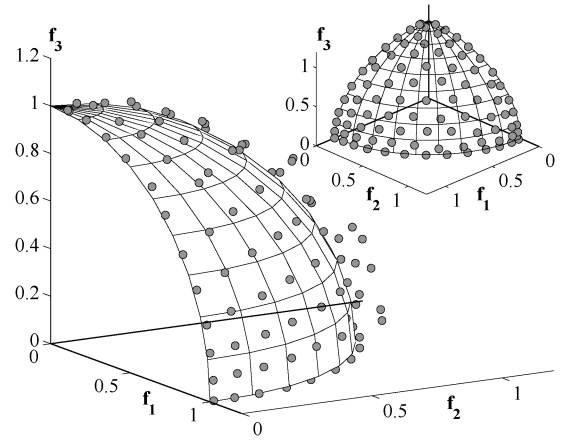


Fig. 19. MOEA/D-PBI solutions on the three-objective WFG6 problem.

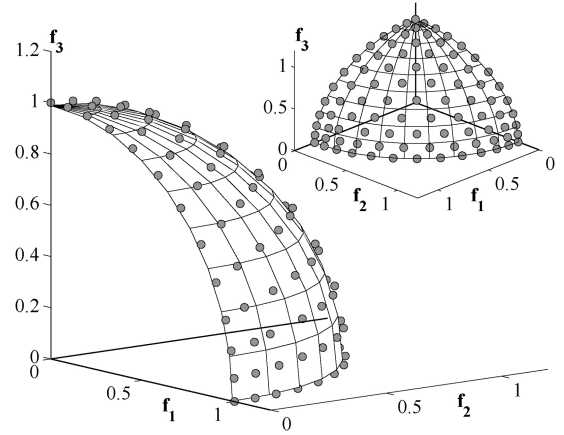


Fig. 20. NSGA-III solutions on the three-objective WFG7 problem.

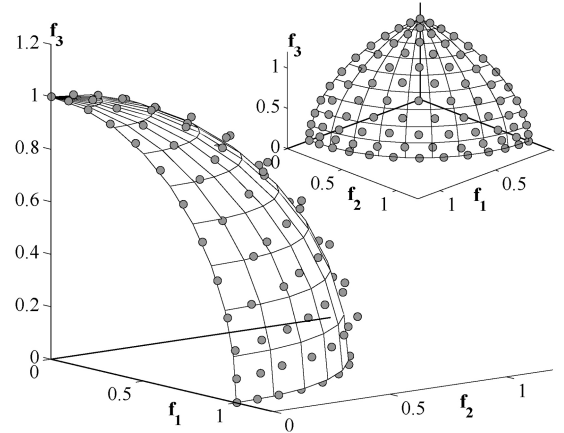


Fig. 21. MOEA/D-PBI solutions on the three-objective WFG7 problem.

DTLZ4 problem), both MOEA/D approaches fail to maintain a good distribution of points, while NSGA-III performs well.

B. Classical Generative Method

For solving many-objective optimization problems, we require a set of reference points—either supplied by the user or systematically constructed as discussed earlier. One may then ponder how the proposed NSGA-III method will compare

TABLE V

IGD VALUES FOR NSGA-III AND MOEA/D-PBI APPROACHES ON THREE- TO 15-OBJECTIVE WFG PROBLEMS

Problem	M	MaxGen	NSGA-III	MOEA/D-PBI
WFG6	3	400	4.828×10^{-3}	1.015×10^{-2}
			1.224×10^{-2}	3.522×10^{-2}
			5.486×10^{-2}	1.066×10^{-1}
	5	750	5.065×10^{-3}	8.335×10^{-3}
			1.965×10^{-2}	4.230×10^{-2}
			4.474×10^{-2}	1.058×10^{-1}
WFG7	8	1500	1.009×10^{-2}	1.757×10^{-2}
			2.922×10^{-2}	5.551×10^{-2}
			7.098×10^{-2}	1.156×10^{-1}
	10	2000	1.060×10^{-2}	9.924×10^{-3}
			2.491×10^{-2}	4.179×10^{-2}
			6.129×10^{-2}	1.195×10^{-1}
	15	3000	1.368×10^{-2}	1.513×10^{-2}
			2.877×10^{-2}	6.782×10^{-2}
			6.970×10^{-2}	1.637×10^{-1}

TABLE VI

BEST, MEDIAN, AND WORST IGD AND CONVERGENCE METRIC VALUES OBTAINED FOR NSGA-III AND CLASSICAL GENERATIVE METHODS FOR THREE-OBJECTIVE DTLZ1 AND DTLZ2 PROBLEMS

Prob.	FE	NSGA-III		Generative Method	
		IGD	GD	IGD	GD
DTLZ1	36,400	4.880×10^{-4}	4.880×10^{-4}	6.400×10^{-2}	1.702×10^1
		1.308×10^{-3}	6.526×10^{-4}	8.080×10^{-2}	1.808×10^1
		4.880×10^{-3}	7.450×10^{-4}	1.083×10^{-1}	1.848×10^1
DTLZ2	22,750	1.262×10^{-3}	1.264×10^{-3}	1.113×10^{-3}	9.678×10^{-5}
		1.357×10^{-3}	1.270×10^{-3}	6.597×10^{-3}	1.019×10^{-4}
		2.114×10^{-3}	1.274×10^{-3}	9.551×10^{-3}	1.082×10^{-4}

with a classical generative method in which multiple scalarized single-objective optimization problems can be formulated for each of the preferred or structured reference points and solved independently. For this purpose, we minimize the PBI-metric for each case. Along the reference direction obtained by joining the ideal point (\mathbf{z}^*) to the supplied reference point ($\bar{\mathbf{z}}$) dictated by a \mathbf{w} -vector [a unit vector $\mathbf{w} = (\bar{\mathbf{z}} - \mathbf{z}^*)/|\bar{\mathbf{z}} - \mathbf{z}^*|$], the distance (d_1) along the \mathbf{w} -direction and the distance (d_2) perpendicular to the \mathbf{w} -direction are computed for any point \mathbf{x} . A weighted sum of these two directions is then minimized as

$$\text{Minimize}_{\mathbf{x}} \quad d_1 + \theta d_2 = \mathbf{w}^T \mathbf{f}(\mathbf{x}) + \theta (\|\mathbf{f}(\mathbf{x}) - \mathbf{w}^T \mathbf{f}(\mathbf{x})\| \mathbf{w}). \quad (6)$$

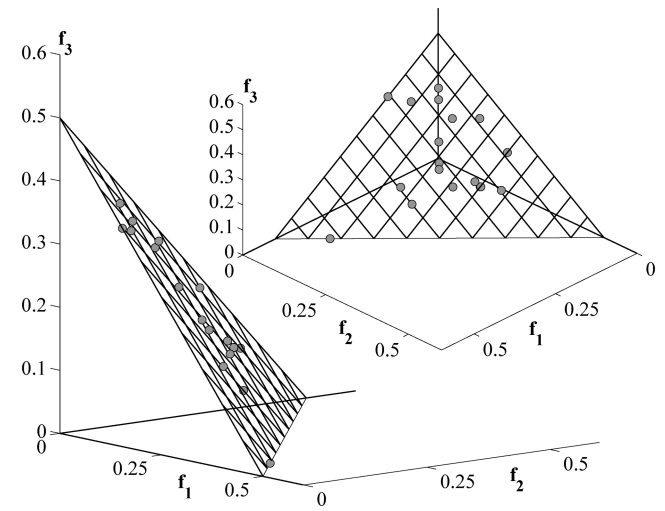


Fig. 22. Solutions obtained by classical generative method for DTLZ1. Only the points obtained close to the true Pareto-optimal front are shown.

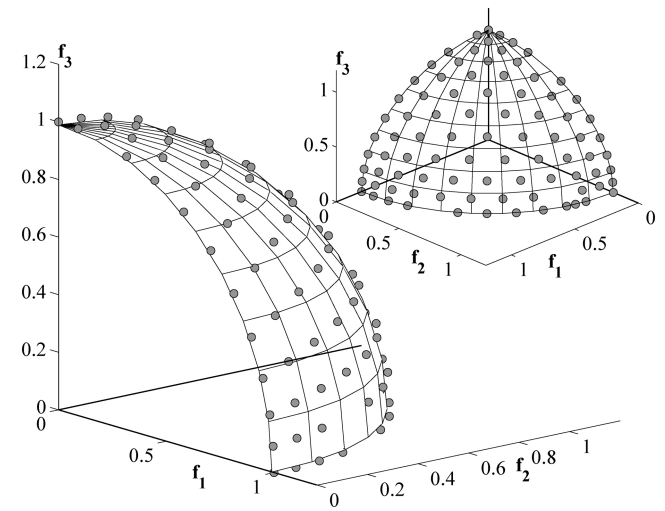


Fig. 23. Solutions obtained by the classical generative method for DTLZ2.

The parameter θ is set to 5 for all reference points [10]. In other words, the above minimization process is likely to find the intersection point between the reference direction \mathbf{w} and the Pareto-optimal surface, if there exists an intersection. Since the ideal point (\mathbf{z}^*) is required to be known for this method, we use the origin to be the ideal vector.

To make a fair comparison, for H reference points we allocate a maximum of $T = F_{\text{ENSGA-III}}/H$ (where $F_{\text{ENSGA-III}}$ is the total number of solution evaluations needed by NSGA-III) function evaluations to each optimization process. For three-objective DTLZ1 and DTLZ2 problems, $F_{\text{ENSGA-III}} = 92 \times 400$ or 36 800 was required to find 91 solutions. Therefore, we allocate 36 800/91 or 405 function evaluations to each optimization run by a fmincon routine of MATLAB. A random solution is used for initialization. Figs. 22 and 23 show the final solutions obtained by this generative method.

The DTLZ1 problem has multiple local fronts and the MATLABs fmincon routine could not find a global Pareto-

TABLE VII

BEST, MEDIAN AND WORST IGD VALUES FOR THREE-OBJECTIVE SCALED DTLZ1 AND DTLZ2 PROBLEMS USING NSGA-III AND MOEA/D ALGORITHMS. A SCALING FACTOR OF 10^{i-1} , $i = 1, 2, \dots, M$, IS USED

Prob.	Max Gen	NSGA-III	MOEA/D -PBI	MOEA/D -TCH
DTLZ1	400	3.853×10^{-4}	2.416×10^{-2}	8.047×10^{-2}
		1.214×10^{-3}	2.054×10^{-1}	2.051×10^{-1}
		1.103×10^{-2}	4.113×10^{-1}	2.704×10^{-1}
DTLZ2	250	1.347×10^{-3}	4.749×10^{-2}	2.350×10^{-1}
		2.069×10^{-3}	3.801×10^{-1}	5.308×10^{-1}
		5.284×10^{-3}	5.317×10^{-1}	5.321×10^{-1}

optimal solution every time with the allotted number of function evaluations. Table VI shows the IGD and GD metric (average distance of obtained points from the closest reference points, a metric opposite in sense to IGD metric) values. For the three-objective DTLZ2 problem, the generative method is able to find a well-distributed set of points, as shown in the figure. However, Table VI indicates that the distribution of points is not as good as that obtained by NSGA-III with the same number of function evaluations. The inherent parallel search of NSGA-III constitutes a more efficient optimization.

C. Scaled Test Problems

To investigate the algorithm's performance on problems that have differently scaled objective values, we consider DTLZ1 and DTLZ2 problems again, but now we modify them as follows. Objective f_i is multiplied by a factor 10^{i-1} . To illustrate, objectives f_1 , f_2 , and f_3 for the three-objective scaled DTLZ1 problem are multiplied by 10^0 , 10^1 , and 10^2 , respectively.

To handle different scaling of objectives and make the distances (d_1 and d_2) along and perpendicular to reference directions in the MOEA/D-PBI approach, we normalize the objective values using the procedure suggested for the MOEA/D-TCH approach in the original MOEA/D study [10]. We also use the code from the MOEA/D website [50] to obtain the points. Figs. 24–26 show the obtained distribution of points using NSGA-III, MOEA/D-PBI, and MOEA/D-TCH approaches, respectively. It is clear that both MOEA/D approaches with objective normalization are not able to handle the scaling involved in the objectives adequately, whereas NSGA-III's operators, normalization of objectives, and the adaptive hyper-plane construction process are able to negotiate the scaling of the objectives quite well. In the scaled problems, IGD metric is computed by first normalizing the objective values using the ideal and nadir points of the exact Pareto-optimal front and then computing the IGD value using the reference points as before. Resulting IGD values are shown in Table VII. Similar performance is also observed for the scaled DTLZ2 problem as shown in Figs. 27–29 and normalized IGD values are tabulated in Table VII.

Next, Table VIII shows the IGD values of the obtained solutions for five-, eight-, ten-, and 15-objective scaled DTLZ1 and

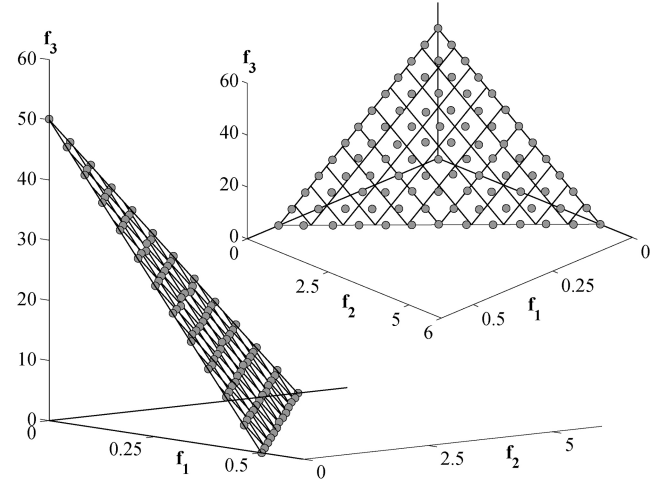


Fig. 24. Obtained solutions by NSGA-III for scaled DTLZ1.

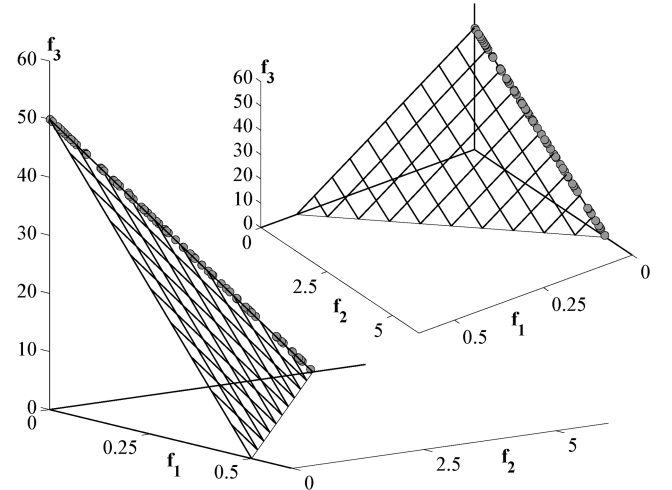


Fig. 25. Obtained solutions by MOEA/D-PBI for scaled DTLZ1.

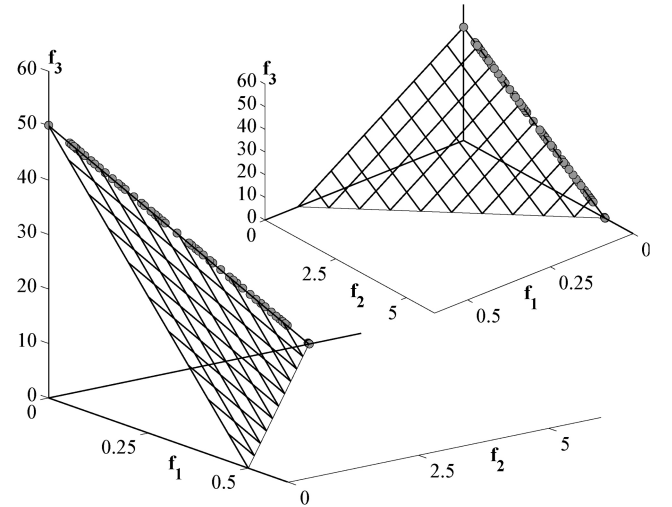


Fig. 26. Obtained solutions by MOEA/D-TCH for scaled DTLZ1.

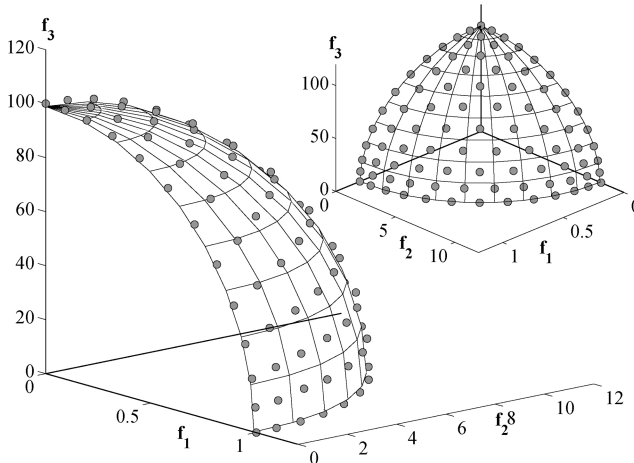


Fig. 27. Obtained solutions by NSGA-III for scaled DTLZ2.

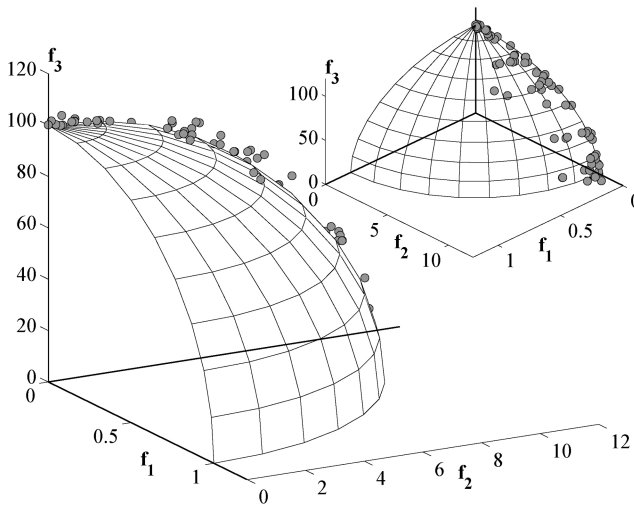


Fig. 28. Obtained solutions by MOEA/D-PBI for scaled DTLZ2.

DTLZ2 problems. Due to the poor performance of MOEA/D algorithms in scaled three-objective problems, we do not apply them further to the above higher-dimensional scaled problems. Although it is difficult to visualize a higher-dimensional front, a small IGD value in each case refers to a well-distributed set of points.

It is interesting to note that the MOEA/D-PBI algorithm that worked so well in the normalized test problems in the previous subsection did not perform well for the scaled version of the same problems. Practical problems are far from being normalized and the objectives are usually scaled differently. An efficient optimization algorithm must handle different scaling of objectives as effectively as shown by NSGA-III.

D. Convex DTLZ2 Problem

The DTLZ1 problem has a linear Pareto-optimal front and DTLZ2 to DTLZ4 problems have concave Pareto-optimal fronts. To investigate the performance of NSGA-III and both versions of MOEA/D on scalable problems having convex Pareto-optimal fronts, we create a new problem based on the DTLZ2 problem. After the objective values (f_i , $i =$

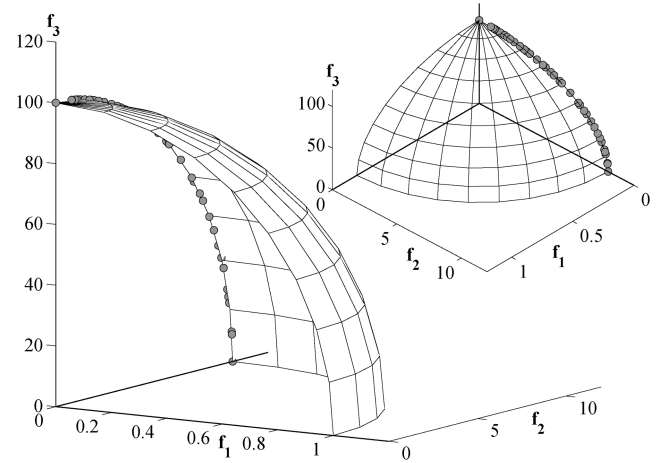


Fig. 29. Obtained solutions by MOEA/D-TCH for scaled DTLZ2.

TABLE VIII
BEST, MEDIAN, AND WORST IGD VALUES FOR SCALED M -OBJECTIVE DTLZ1 AND DTLZ2 PROBLEMS

Problem	M	Scaling factor	MaxGen	NSGA-III
DTLZ1	3	10^i	400	3.853×10^{-4} 1.214×10^{-3} 1.103×10^{-2}
	5	10^i	600	1.099×10^{-3} 2.500×10^{-3} 3.921×10^{-2}
	8	3^i	750	4.659×10^{-3} 1.051×10^{-2} 1.167×10^{-1}
	10	2^i	1000	3.403×10^{-3} 5.577×10^{-3} 3.617×10^{-2}
	15	1.2^i	1500	3.450×10^{-3} 6.183×10^{-3} 1.367×10^{-2}
DTLZ2	3	10^i	250	1.347×10^{-3} 2.069×10^{-3} 5.284×10^{-3}
	5	10^i	350	1.005×10^{-2} 2.564×10^{-2} 8.430×10^{-2}
	8	3^i	500	1.582×10^{-2} 1.788×10^{-2} 2.089×10^{-2}
	10	3^i	750	2.113×10^{-2} 3.334×10^{-2} 2.095×10^{-1}
	15	2^i	1000	2.165×10^{-2} 2.531×10^{-2} 4.450×10^{-2}

$1, 2, \dots, M$) are computed using the original DTLZ2 objective functions, we map them as

$$f_i \leftarrow f_i^4 \quad i = 1, 2, \dots, (M-1)$$

$$f_M \leftarrow f_M^2.$$

The Pareto-optimal surface is then given as

$$f_M + \sum_{i=1}^{M-1} \sqrt{f_i} = 1. \quad (7)$$

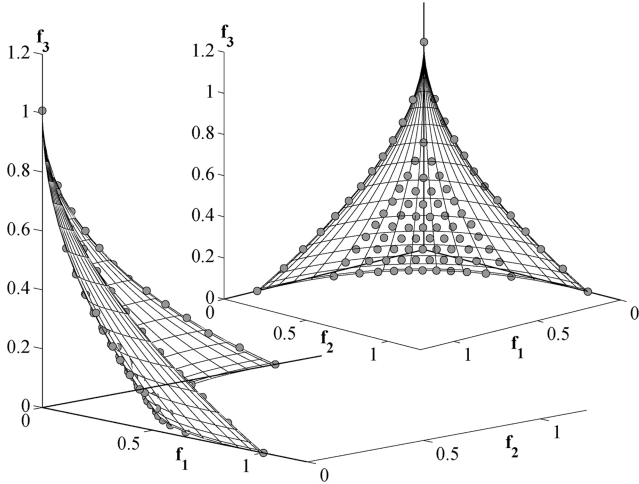


Fig. 30. Obtained solutions by NSGA-III for the convex Pareto-optimal front problem.

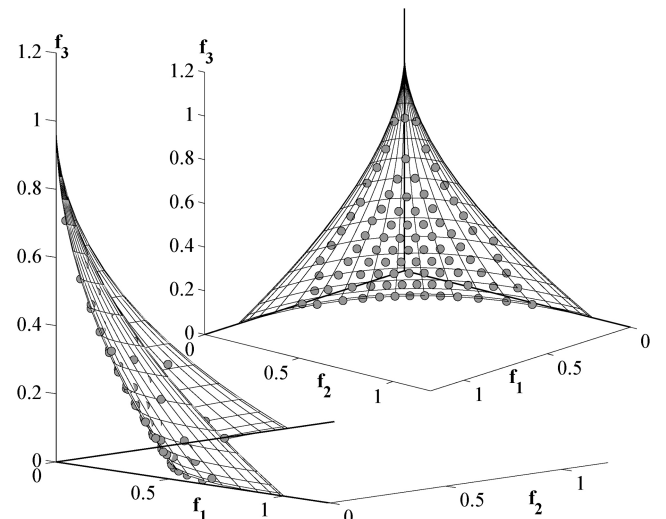


Fig. 31. Obtained solutions by MOEA/D-PBI for the convex Pareto-optimal front problem.

Fig. 30 shows the obtained points on a three-objective convex Pareto-optimal front problem with $H = 91$ reference points. As the figure shows, the Pareto-optimal surface is almost flat at the edges, but changes sharply in the intermediate region. Although the reference points are uniformly placed on a normalized hyper-plane making an equal angle to all objective axes, the distribution of points on the Pareto-optimal front does not come out to be uniform. Despite such a nature of the front, NSGA-III is able to find a widely distributed set of points on the edges and also in the intermediate region of the surface. Note that the range of each objective for the Pareto-optimal set is identical (within $[0, 1]$); hence, MOEA/D-PBI is expected to perform well. As shown in Fig. 31, a nicely distributed set of points is found in the middle part of the front, but the algorithm fails to find points on the boundary of the Pareto-optimal front. This is due to a small slope of the surface at the boundary region. The use of penalty parameter value $\theta = 5$ finds a nonboundary point to have a better PBI metric value for the boundary reference directions. A larger value of θ may allow MOEA/D-PBI to find the exact boundary points, thereby requiring doing another parametric study with θ . However, the advantage of parameter-less approach in NSGA-III is clear from this problem. MOEA/D-TCH performs poorly again, as shown in Fig. 32.

Table IX shows the best, median, and worst IGD values of 20 independent runs [obtained using (5)] for all three methods. Clearly, NSGA-III performs the best by finding a set of points having an order of magnitude smaller IGD values in three-, five-, eight-, ten-, and 15-objective versions of the convex DTLZ2 problem.

To demonstrate the distribution of obtained points on a higher-objective problem, we show the obtained points of the median performed run of the 15-objective convex DTLZ2 problem on value path plots using NSGA-III and MOEA/D-PBI approaches in Figs. 33 and 34, respectively. It is clear from the plots that NSGA-III is able to find a good spread of solutions in the entire range of Pareto-optimal front

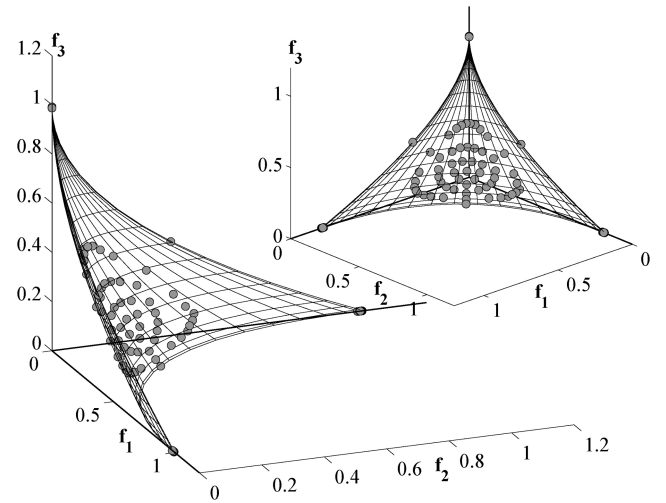


Fig. 32. Obtained solutions by MOEA/D-TCH for the convex Pareto-optimal front problem.

TABLE IX
BEST, MEDIAN, AND WORST IGD VALUES FOR THE
CONVEX DTLZ2 PROBLEM

M	MaxGen	NSGA-III	MOEA/D-PBI	MOEA/D-TCH
3	250	2.603×10^{-3}	3.050×10^{-2}	6.835×10^{-2}
		4.404×10^{-3}	3.274×10^{-2}	6.871×10^{-2}
		8.055×10^{-3}	3.477×10^{-2}	6.912×10^{-2}
5	750	7.950×10^{-3}	1.082×10^{-1}	1.211×10^{-1}
		1.341×10^{-2}	1.103×10^{-1}	1.223×10^{-1}
		1.917×10^{-2}	1.117×10^{-1}	1.235×10^{-1}
8	2000	2.225×10^{-2}	2.079×10^{-1}	2.235×10^{-1}
		2.986×10^{-2}	2.086×10^{-1}	2.396×10^{-1}
		4.234×10^{-2}	2.094×10^{-1}	2.490×10^{-1}
10	4000	7.389×10^{-2}	2.117×10^{-1}	2.373×10^{-1}
		9.126×10^{-2}	2.119×10^{-1}	2.472×10^{-1}
		1.051×10^{-1}	2.120×10^{-1}	2.514×10^{-1}
15	4500	2.169×10^{-2}	3.681×10^{-1}	3.851×10^{-1}
		2.769×10^{-2}	3.682×10^{-1}	3.911×10^{-1}
		4.985×10^{-2}	3.683×10^{-1}	3.972×10^{-1}

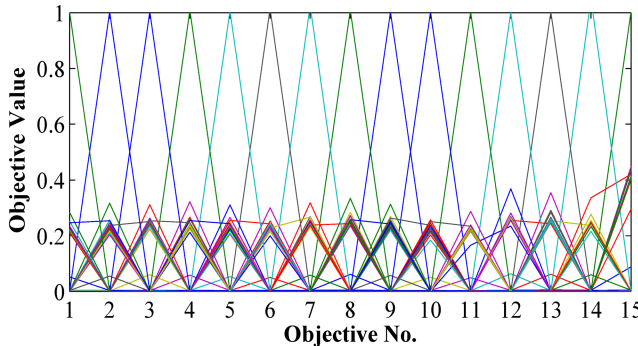


Fig. 33. NSGA-III solutions are shown using 15-objective value path format for the convex problem.

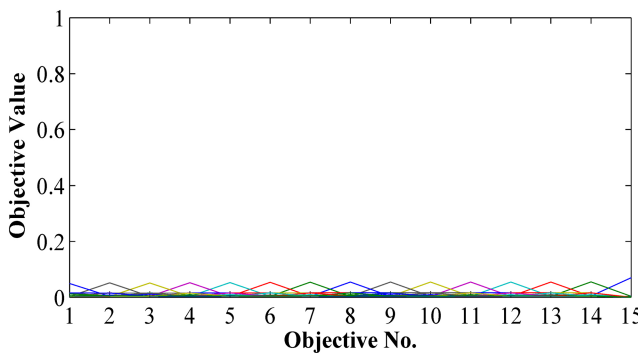


Fig. 34. MOEA/D-PBI solutions are shown using ten-objective value path format for the convex problem.

$(f_i \in [0, 1] \text{ for all } i)$, but MOEA/D-PBI is unable to find solutions having larger objective values.

Before we evaluate the proposed NSGA-III approach further, we highlight a couple of properties of MOEA/D-TCH and MOEA/D-PBI approaches that become clear from the simulation results above.

- 1) As observed in three-objective results with MOEA/D-TCH above (Fig. 7, for example), it ends up generating a nonuniform distribution of points. This is due to the way the Tchebycheff metric is constructed. Moreover, multiple weight vectors produce an identical extreme solution, thereby wasting computational efforts.
- 2) Interestingly, although we have not demonstrated it here, MOEA/D-PBI is potentially capable of generating dominated solutions depending on the parameter θ . This could cause MOEA/D-PBI approach to make a waste of computational effort in carrying dominated solutions.

Although special care can be taken to reduce the chance of above, they are important for one to be aware while working with MOEA/D-PBI or MOEA/D-TCH approaches.

VI. FURTHER INVESTIGATIONS OF NSGA-III

Having performed well on all test problems in the above sections, we now investigate NSGA-III's performance in certain special types of many-objective problem-solving tasks.

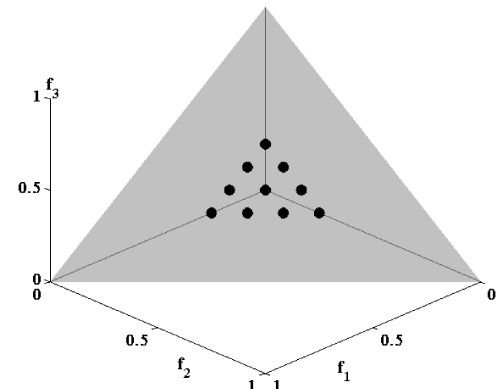


Fig. 35. Reference points used for Scenario 1 on normalized hyper-plane.

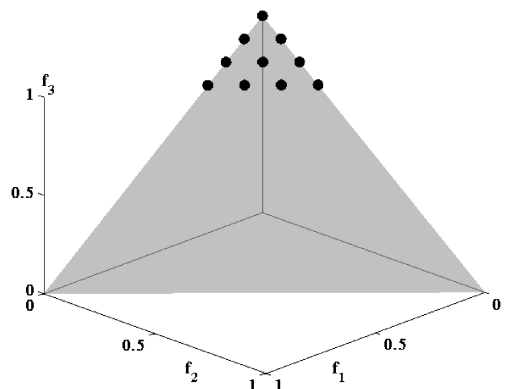


Fig. 36. Reference points used for Scenario 2 on normalized hyper-plane.

A. Finding a Preferred Part of Pareto-Front

In many-objective optimization problems, the user may not always be interested in finding the entire Pareto-optimal front. Practically speaking, a user is often interested in a particular preferred part of the Pareto-optimal front. In such a scenario, the user may represent his/her preferred region using a few representative reference points (or aspiration points). The aim in such a many-objective optimization task is to find Pareto-optimal points that are in some sense closest to the supplied reference points.

Recall from Section IV-B that the proposed NSGA-III algorithm can also be applied with a set of H user-supplied reference points, instead of Das and Dennis's structured reference points used so far. Here, we demonstrate the working of NSGA-III for scaled DTLZ1 and DTLZ2 problems for a few user-supplied preference information. In such a case, in order to determine the right normalized hyper-plane, by default we also supply M additional reference points, one at each objective axis at an intercept of unity. The presence of these extreme points will attempt to keep extreme Pareto-optimal points, thereby forming a proper normalized hyper-plane needed to have appropriate scaling of the objectives.

For both scaled three-objective DTLZ1 and DTLZ2 problems, we supply ten reference points in the middle of the normalized hyper-plane (scenario 1, as shown in Fig. 35). As mentioned, three additional reference points $(1, 0, 0)^T$, $(0, 1, 0)^T$, and $(0, 0, 1)^T$, are also included for the execution of

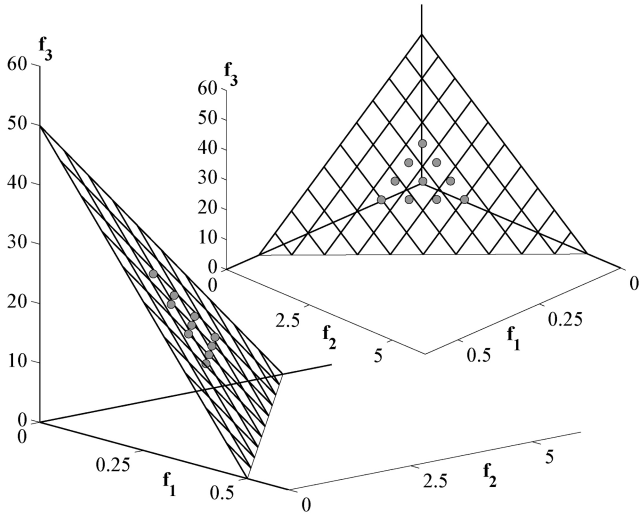


Fig. 37. Preferred solutions (scenario 1) obtained by NSGA-III for three-objective DTLZ1.

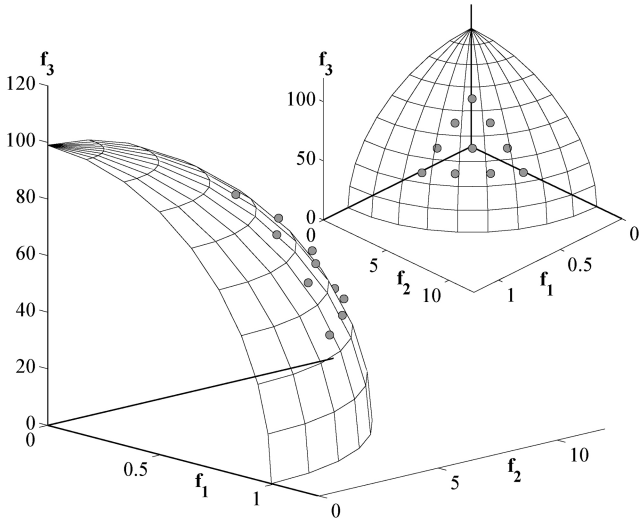


Fig. 38. Preferred solutions (scenario 1) obtained by NSGA-III for three-objective DTLZ2.

the algorithm, thereby making a total of 13 supplied reference points. Fig. 37 shows the points (without the extreme points) obtained by NSGA-III on the scaled Pareto-optimal front of the DTLZ1 problem. Fig. 38 shows ten obtained points for the scaled DTLZ2 problem for scenario 1. Next, we supply a set of ten reference points on a different part of the normalized hyper-plane, as shown as scenario 2 in Fig. 36. Fig. 38 shows the obtained points on the scaled DTLZ2 problem. In both cases, a set of ten near-Pareto-optimal points are obtained close to where the reference points were supplied.

Best, median, and worst IGD values for the obtained points for three-objective and ten-objective scaled DTLZ1 and DTLZ2 problems are shown in Table X. The IGD values are computed by normalizing the obtained objective values by the theoretical ideal and nadir points and by projecting ten supplied reference points on the normalized Pareto-optimal front. A small IGD value in each case ensures the convergence and diversity of the obtained solutions. The success of NSGA-III in

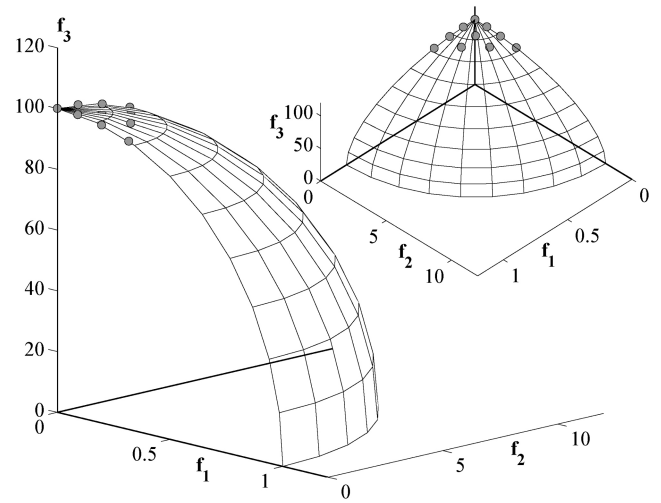


Fig. 39. Preferred solutions (scenario 2) obtained by NSGA-III for three-objective DTLZ2.

TABLE X
BEST, MEDIAN, AND WORST IGD VALUES FOR SCALED DTLZ1 AND DTLZ2 PROBLEMS WITH TEN REFERENCE POINTS

Function	<i>M</i>	<i>N</i>	MaxGen	NSGA-III
DTLZ1	3	28	750	4.945×10^{-4}
				4.076×10^{-3}
(Scenario 1) (Figure 35)	10	100	2000	1.898×10^{-2}
				1.671×10^{-3}
DTLZ1	3	28	750	5.792×10^{-3}
				1.212×10^{-1}
(Scenario 2) (Figure 36)	10	100	2000	2.742×10^{-4}
				2.875×10^{-3}
DTLZ2	3	28	250	1.741×10^{-2}
				4.194×10^{-3}
(Scenario 1) (Figure 35)	10	100	1500	7.393×10^{-3}
				5.799×10^{-2}
DTLZ2	3	28	250	6.459×10^{-4}
				1.473×10^{-3}
(Scenario 2) (Figure 36)	10	100	1500	3.883×10^{-3}
				2.840×10^{-3}
DTLZ2	3	28	250	1.327×10^{-3}
				2.706×10^{-3}
(Scenario 2) (Figure 36)	10	100	1500	8.099×10^{-3}
				1.576×10^{-2}
DTLZ2	3	28	250	2.548×10^{-2}
				5.893×10^{-2}

finding just ten Pareto-optimal points on ten-objective scaled problems indicates its potential use in finding a handful of preferred solutions in a many-objective practical optimization problem.

B. Randomly Generated Preferred Reference Points

The supplied preferred reference points considered in the previous subsection are structured. In fact, they were created using Das and Dennis's [48] structured reference point creation procedure. Here, we investigate NSGA-III's ability to deal with a set of randomly created reference points. The procedure used here is the same as in the previous subsection—*M* additional

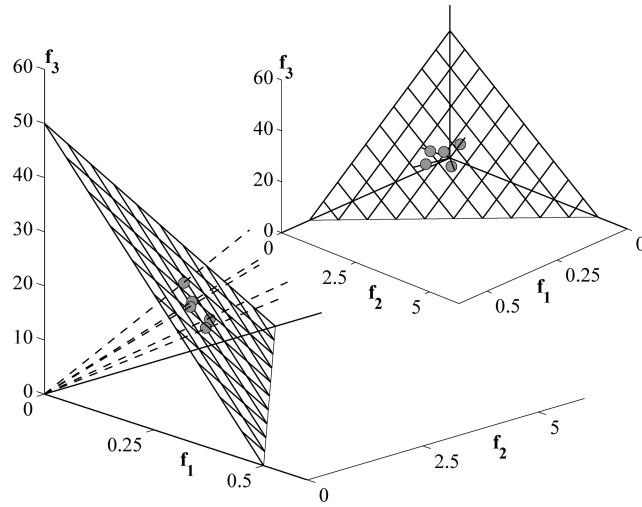


Fig. 40. Preferred solutions obtained by NSGA-III for three-objective DTLZ1.

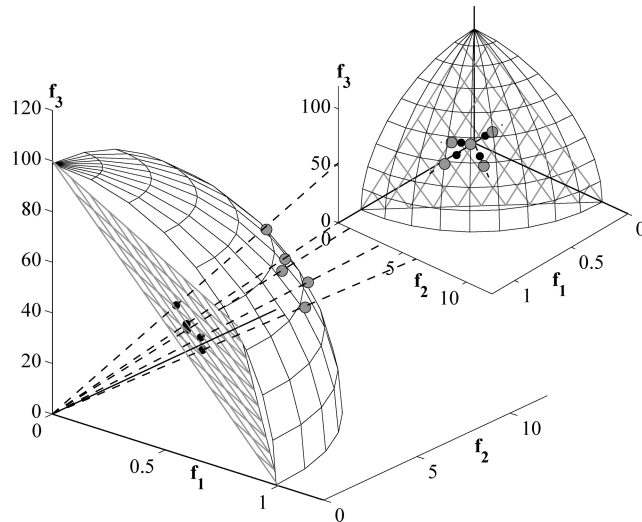


Fig. 41. Preferred solutions obtained by NSGA-III for three-objective DTLZ2.

axis points are included as before for NSGA-III to adaptively create its hyper-plane.

For decision-making purposes, only a few trade-off points can be analyzed, even for a many-objective problem. Here, we investigate if the proposed NSGA-III is able to find only five Pareto-optimal points in a preferred region for three-objective and ten-objective scaled DTLZ1 and DTLZ2 problems. Five random points are supplied in the intermediate region of the normalized hyper-plane (within $z_i \in [0.4, 0.6]$ for all i). Figs. 40 and 41 show the obtained points on scaled three-objective DTLZ1 and DTLZ2 problems, respectively.

Table XI shows the IGD values for three-objective and ten-objective problems. In each case, a small IGD value indicates that NSGA-III is adequate to successfully find the desired solutions.

This application shows promise in applying NSGA-III to many-objective problems (ten-objective or like) with a handful

TABLE XI
BEST, MEDIAN, AND WORST IGD VALUES FOR SCALED DTLZ1 AND DTLZ2 PROBLEMS WITH RANDOMLY SUPPLIED REFERENCE POINTS

Problem	M	N	MaxGen	NSGA-III
DTLZ1	3	28	600	1.621×10^{-3}
				9.870×10^{-3}
	10	100	2000	3.186×10^{-1}
				3.244×10^{-3}
DTLZ2	3	28	250	8.227×10^{-3}
				1.688×10^{-2}
	10	100	1500	5.763×10^{-4}
				1.951×10^{-3}

TABLE XII
MINIMUM POPULATION SIZE AND BEST, MEDIAN AND WORST IGD VALUES OF THE OBTAINED SOLUTIONS FOR THE SCALED DTLZ2 PROBLEM

M	(p^B, p^I)	H	MaxGen	N	NSGA-III
3	(3,0)	10	250	12	4.206×10^{-3}
					1.524×10^{-1}
					1.464×10^{-3}
5	(2,1)	20	500	20	8.537×10^{-3}
					4.952×10^{-3}
					1.195×10^{-1}
10	(2,1)	65	1,000	68	8.641×10^{-3}
					1.155×10^{-2}
					1.842×10^{-2}

(five or like) of preferred reference points—a matter that is of great importance to practitioners.

C. Small Population Size

Previous subsections have shown that NSGA-III can work with a small number of reference points in order to find a few Pareto-optimal points in a preferred region. In previous sections, we have used a population size that is almost equal to the number of reference points. A natural question then arises, “Can NSGA-III work well with a small population size?” We investigate this aspect here.

Table XII tabulates the number of reference points (H) and corresponding layer-wise p and the maximum number of generations considered for different many-objective DTLZ2 problems. We perform this paper for three-, five-, and ten-objective scaled DTLZ2 problems. Identical scaling factors as those shown in Table VIII are used here.

In each case, the population size (N) is always kept as the smallest multiple of four, but greater than the number of reference points (H). A larger number of generations is kept for higher objective problems. The chosen maximum number of generations are also tabulated in the table.

For the three-objective DTLZ2 problem, when we are interested in finding ten well distributed Pareto-optimal points, we find that a population of size 12 is adequate to find all ten Pareto-optimal points after 250 generations (Fig. 42). For the ten-objective problem, if we desire 65 reference points (with

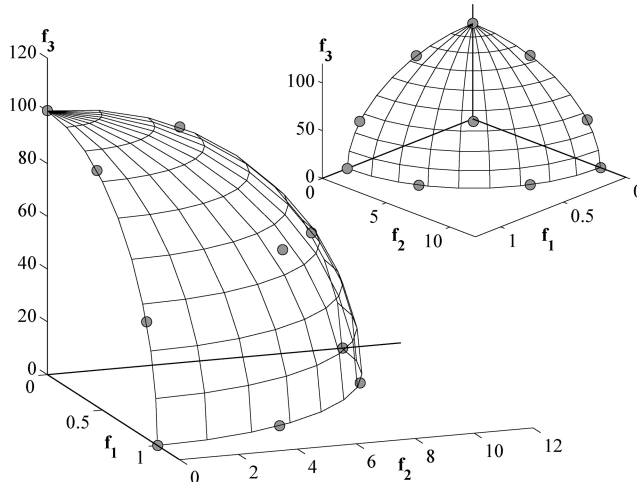


Fig. 42. Obtained points using NSGA-III for the scaled DTLZ2 with a small population size of 12.

two intermediate layers: boundary $p^B = 2$ and intermediate $p^I = 1$), we find that a population of size 68 is adequate to find all 65 solutions after 1000 generations. The best, median, and worst IGD values are shown in the table for three-, five-, and ten-objective DTLZ2 problems. These results show that NSGA-III can work with a small population size at least on DTLZ2 problem due to its focus and balanced emphasis for finding near Pareto-optimal points corresponding to a supplied set of reference points.

D. Nadir Point Estimation

In multiobjective optimization problems, the nadir point is important to be found for various reasons. A nadir point is constructed from the worst objective values for the entire Pareto-optimal set. Thus, along with the ideal point, the nadir point can be used to normalize the objective functions for a systematic and reliable execution of many classical and nonclassical optimization methods. In [54], a nadir point estimation strategy was proposed based on a bilevel evolutionary approach. In that study, three-objective to 20-objective DTLZ1 and DTLZ2 problems were considered for estimating the nadir point. Since studies in the previous two subsections have shown amply that NSGA-III can be used to find a few Pareto-optimal solutions even in ten-objective problems, here we apply NSGA-III to find only the extreme Pareto-optimal points so that the nadir point can be estimated accurately and in a computationally fast manner.

For this purpose, we suggest using M reference points, one on each objective axis, located at unity. We apply NSGA-III to three-objective to 20-objective DTLZ1 and DTLZ2 problems and record the overall function evaluations needed to find the true nadir point with the following termination condition. When the error value (E) computed as

$$E = \sqrt{\sum_{i=1}^M \left(\frac{z_i^{\text{nad}} - z_i^{\text{est}}}{z_i^{\text{nad}} - z_i^*} \right)^2} \quad (8)$$

is less than a threshold (0.01, used here), the run is terminated. Here, \mathbf{z}^* , \mathbf{z}^{nad} , and \mathbf{z}^{est} are the ideal point, the true nadir

TABLE XIII
NADIR POINT ESTIMATION BY NSGA-III IN THREE-OBJECTIVE TO 20-OBJECTIVE DTLZ1 AND DTLZ2 PROBLEMS

Problem	M	N	NSGA-III	NSGA-II [54]
DTLZ1	3	20	7,400 16,660 72,180 45,700	18,800 26,500 45,700
	5	20	25,000 62,900 152,040 58,400 107,100	35,300 274,200 358,000
	10	40	58,640 259,760 483,880 239,800	239,800 274,200 358,000
	15	60	356,460 589,140 1,200,000 750,000 1,100,000 1,800,000	750,000 1,100,000 1,800,000
	20	80	274,800 956,960 1,600,000 2,600,000	2,600,000 3,500,000 4,000,000
DTLZ2	3	20	1,368 1,920 2,532 4,100 4,900 5,500	4,100 4,900 5,500
	5	20	4,320 6,900 13,000 9,400 11,400 14,200	9,400 11,400 14,200
	10	40	31,400 52,840 76,080 77,600 92,800 128,000	77,600 92,800 128,000
	15	60	153,540 213,060 316,860 346,500 429,000 810,000	346,500 429,000 810,000
	20	80	309,440 589,520 734,400 1,089,000 1,415,000 2,102,000	1,089,000 1,415,000 2,102,000

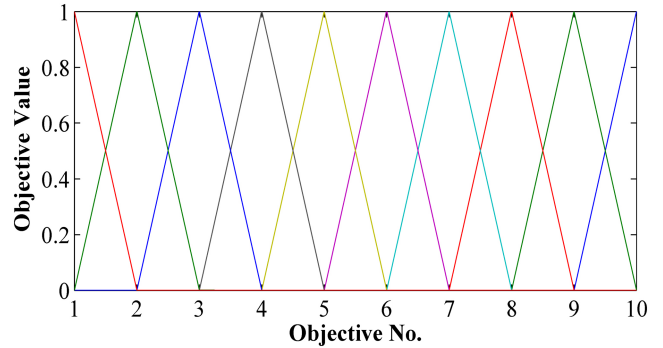


Fig. 43. Value path plot for the ten-objective DTLZ2 problem shows that NSGA-III is able to find the extreme objective values (zero and one) in each objective.

point, and the estimated nadir point by NSGA-III, respectively. Table XIII presents the results and compares them with the evaluations needed to find the nadir point with an identical termination condition in the previous study [54]. In most cases, NSGA-III requires a smaller number of function evaluations than the previous procedure to locate the nadir point reliably.

Fig. 43 shows the value path plot of obtained points for estimating the nadir point for the ten-objective DTLZ2 problems. Understandably, the points near the extreme of the Pareto-optimal front are found. From this plot, the nadir point of the problem is estimated to be $(1, 1, 1, 1, 1, 1, 1, 1, 1, 1)^T$.

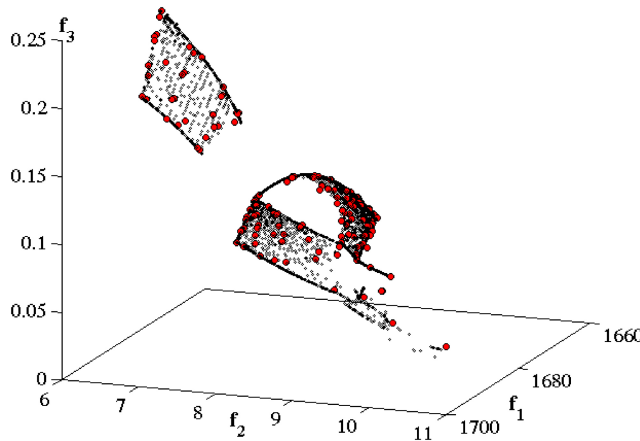


Fig. 44. Sixty solutions are found on the entire front on the three-objective crush-worthiness problem.

VII. TWO PROBLEMS FROM PRACTICE

After solving a number of test problems, we now apply NSGA-III to a couple of engineering design optimization problems. The first problem has three objectives and the second one has nine objectives.

A. Crash-Worthiness Design of Vehicles for Complete Trade-Off Front

This problem aims at optimization of the frontal structure of vehicle for crash-worthiness [55]. The thickness of five reinforced members around the frontal structure is chosen as design variables, while mass of vehicle, deceleration during the full frontal crash (which is proportional to biomechanical injuries caused to the occupants), and toe board intrusion in the offset-frontal crash (which accounts for the structural integrity of the vehicle) are taken as objectives. Mathematical formulation for the three objectives can be found in the original study [55].

All objectives are to be minimized. For this problem, we choose $p = 16$ so that there are $H = \binom{3+16}{16}$ or 153 structured reference points. The reference points are initialized on the entire normalized hyper-plane in the three-objective space. NSGA-III is applied with 156 population size and run for 200 generations. Other parameters are the same as before. Fig. 44 shows the obtained points with an open circle. The nonuniform scaling of objectives is clear from the figure. Although 153 reference points were used, only 60 of them have representative solutions on the final front. The other 93 reference do not correspond to any Pareto-optimal point, thereby indicating discontinuities and holes in the Pareto-optimal front. The ideal point (\mathbf{z}^*) and the nadir point (\mathbf{z}^{nad}) are also estimated from the obtained front.

To investigate the nature of the true Pareto-optimal front, we next create 7381 reference points $\mathbf{z}^{\text{ref},i}$ ($i = 1, \dots, 7381$) with $p = 120$. Using the ideal and nadir points obtained as above, we normalize the objectives and then solve the achievement scalarization function (ASF) [56] corresponding to each weight vector $\mathbf{w}^i = \mathbf{z}^{\text{ref},i}$. Each ASF is minimized using MATLABs fmincon routine. The resulting 7381 points are

collected and dominated points are removed. We noticed that only 4450 points remain nondominated. These nondominated points are shown in Fig. 44 with a dot. It is clear that the NSGA-III obtained set of 60 points are widely distributed on the entire front spanned by points obtained using a classical generating method, but using only a fraction of the overall computational effort. Interestingly, 4450 trade-off points reveal the complex nature of Pareto-optimal front (having holes and varying density of points) for this practical problem and the ability of NSGA-III to find a few widely distributed points on the entire front.

To investigate the closeness of NSGA-III points with the classically optimized solutions, we compute the convergence metric (average distance of NSGA-III points from the closest fmincon-optimized points) and the minimum, median, and maximum convergence metric values are found to be 0.0019, 0.0022, and 0.0026, respectively. Since these values are small, they indicate that obtained NSGA-III solutions are close to the classically optimized front. This problem demonstrates the use of NSGA-III in finding a representative set of points near the entire Pareto-optimal front on problems having practical difficulties (such as differences in scaling of objectives and potential holes in the Pareto-optimal front).

B. Car Cab Design With Preference Information

Next, we consider a vehicle performance optimization problem having 11 decision variables involving dimensions of the car body and bounds on natural frequencies. The problem involves nine objectives on roominess of the car, fuel economy, acceleration time, and road noise at different speeds. A mathematical formulation can be found elsewhere [57].

In this problem, we demonstrate NSGA-III's ability to use preference information in finding a few preferred nondominated solutions on a part of the Pareto-optimal front, instead of on the complete front. We apply NSGA-III with only ten reference points in the intermediate part of the Pareto-optimal front. For this purpose, we first create ten random points on the entire unit hyper-plane and then shrink them within 25% around the centroid of the unit hyper-plane. As suggested in Section VI-A, nine extreme reference points are also included for a better normalization purpose. A population of size 100 is used and NSGA-III is run for 4000 generations. Twenty independent runs are made with different sets of reference points and resulting solutions are compared with the classical achievement scalarizing function approach implemented with MATLABs fmincon routine. To have good representative solutions in the chosen intermediate part, the fmincon routine is run for 20 000 random reference points initialized in the same intermediate range one at a time. A domination check of final solutions makes 11 280 of them nondominated to each other. Each set of ten solutions from NSGA-III runs is then compared against these 11 280 fmincon solutions and the GD metric value is computed. The solutions from the specific NSGA-III run corresponding to the median GD metric value are shown against the silhouette of 11 280 fmincon solutions on a value path plot in Fig. 45 to make a visual comparison. The trade-off information and spread of obtained NSGA-III solutions are clear from the plot. While the large number of fmincon

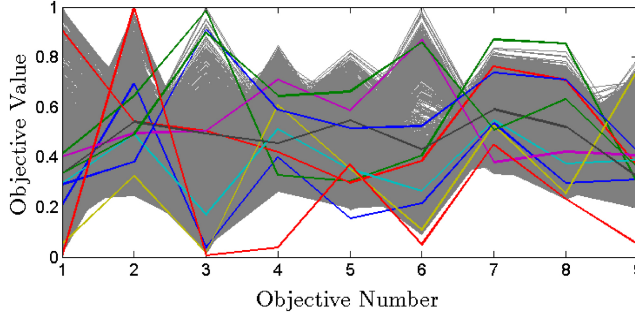


Fig. 45. Value path plot for the nine-objective car cab design problem shows that NSGA-III is able to find as few as ten preferred solutions within the silhouette of solutions found by classical means.

solutions provide a range of objective values for the chosen range of reference points, only one out of ten NSGA-III solutions has two objective values (f_4 and f_9) outside the range. The nine other solutions quite nicely represent the relevant part of the Pareto-optimal front. With NSGA-III's ability to find just ten preferred trade-off solutions on a nine-objective non-dominated front should remain as a significant step toward a convenient post-optimal multicriterion decision-making task.

To quantify the convergence of NSGA-III solutions, the best, median, and worst GD metric values against 11 280 fmincon solutions on the normalized objective space are computed as 0.0245, 0.0408, and 0.0566. These values are small enough to indicate the closeness of obtained NSGA-III solutions from the fmincon solutions. The ability of NSGA-III to find a handful of trade-off points in a preferred part of a nine-objective practical optimization problem having different scaling of objectives shows a promise of its use in practical many-objective optimization problems.

VIII. CONCLUSION

In this paper, we have suggested a reference point based approach to an earlier-proposed NSGA-II framework for solving many-objective optimization problems. The proposed NSGA-III approach has been applied to three-objective to 15-objective existing and new test problems and to three-objective and nine-objective practical problems. The test problems involve fronts that have convex, concave, disjointed, differently scaled, biased density of points across the front, and multimodality involving multiple local fronts to which an optimization algorithm can get stuck. In all such problems, the proposed NSGA-III approach has been able to successfully find a well-converged and well-diversified set of points repeatedly over multiple runs. The performance scaling to 15 objectives is achieved mainly due to the aid in diversity preservation by supplying a set of well-distributed reference points. In higher-dimensional problems, EMO algorithms face with an increasingly difficult task of maintaining diversity, as well as in converging to the Pareto-optimal front. The supply of a set of reference points and NSGA-III's efficient niching methodology in finding a Pareto-optimal solution associated with each reference point has made the diversity

preservation of obtained solutions in as large as 15 objectives possible.

The performance of NSGA-III has been compared with several versions of a recently proposed MOEA/D procedure. Although different MOEA/Ds have shown their working on different problems, no single version is able to solve all problems efficiently. Having solved all problems well by the proposed NSGA-III procedure, there is another advantage of it that is worth mentioning here. Unlike MOEA/D versions, the NSGA-III procedure does not require any additional parameter to be set.

Furthermore, NSGA-III has been tested for its ability to solve a number of different types of many-objective problem-solving tasks. It has been demonstrated that NSGA-III is able to work with a small number of user-supplied structured or randomly assigned reference points, thereby making the method suitable for a many-objective preference-based optimization-cum-decision-making approach. It has also been shown that the NSGA-III procedure can be used to quickly estimate the nadir point in many-objective optimization problems, compared to another EMO-based method proposed earlier. For a practical application, only a handful of trade-off points are required for decision-making in multiobjective and many-objective optimization problems. It has been shown that NSGA-III can be used to find only a few points (20 in five-objective and 65 in a ten-objective problem) with a small population size, thereby reducing the computational efforts.

The proposed NSGA-III approach with a supply of a set of reference points has a similar implicit principle to the hyper-grid-based archiving techniques, such as adaptive grid algorithm [58], [59] and ϵ -MOEA [60], [61]. Grid-based methods require exponentially more grids to be considered with an increase in objectives, whereas ϵ -domination concept, although reducing the burden of finding an appropriate diversity in solutions somewhat, still poses enough difficulties in finding well-distributed Pareto-optimal solutions for a large-dimensional problem. However, it remains an interesting future study to compare NSGA-III's performance with an ϵ -domination-based algorithm for many-objective optimization problems. NSGA-III's performance has been found to be much better than a classical generating method in many-objective problems here. However, a more thorough study using population-based aggregation methods [62], [63] in which multiple search directions are used simultaneously is worth pursuing.

Results of many different problems with box constraints used in this paper have clearly shown promise for NSGA-III's further application in other challenging problems. In the sequel of this paper [52], we have extended NSGA-III to solve constrained many-objective optimization problems that have generic inequality and equality constraints and also suggested an adaptive NSGA-III approach for adding and deleting the supplied reference points adaptively to maximize the number of obtained Pareto-optimal solutions in a computationally efficient manner. Nevertheless, this paper has addressed the issues and difficulties related to solving many-objective optimization problems, reviewed some past studies in this direction, suggested a viable many-objective evolutionary algorithm, and

demonstrated proof-of-principle results on many problems including two engineering design problems.

REFERENCES

- [1] O. Chikumbo, E. Goodman, and K. Deb, "Approximating a multi-dimensional Pareto front for a land use management problem: A modified MOEA with an epigenetic silencing metaphor," in *Proc. CEC-2012*, pp. 1–8.
- [2] C. A. Coello Coello and G. B. Lamont, *Applications of Multi-Objective Evolutionary Algorithms*. Singapore: World Scientific, 2004.
- [3] K. Deb, *Multi-Objective Optimization Using Evolutionary Algorithms*. Chichester, U.K.: Wiley, 2001.
- [4] K. Deb and D. Saxena, "Searching for Pareto-optimal solutions through dimensionality reduction for certain large-dimensional multi-objective optimization problems," in *Proc. WCCI-2006*, pp. 3352–3360.
- [5] K. Deb, S. Agrawal, A. Pratap, and T. Meyarivan, "A fast and elitist multi-objective genetic algorithm: NSGA-II," *IEEE Trans. Evol. Comput.*, vol. 6, no. 2, pp. 182–197, Apr. 2002.
- [6] E. Zitzler, M. Laumanns, and L. Thiele, "SPEA2: Improving the strength Pareto evolutionary algorithm for multiobjective optimization," in *Evolutionary Methods for Design Optimization and Control With Applications to Industrial Problems*, K. C. Giannakoglou, D. T. Tsahalis, J. Périoux, K. D. Papailiou, and T. Fogarty, Eds. Athens, Greece: International Center for Numerical Methods in Engineering (CIMNE), 2001, pp. 95–100.
- [7] E. Zitzler and L. Thiele, "Multiobjective evolutionary algorithms: A comparative case study and the strength Pareto approach," *IEEE Trans. Evol. Comput.*, vol. 3, no. 4, pp. 257–271, Nov. 1999.
- [8] E. Zitzler, L. Thiele, M. Laumanns, C. M. Fonseca, and V. G. Fonseca, "Performance assessment of multiobjective optimizers: An analysis and review," *IEEE Trans. Evol. Comput.*, vol. 7, no. 2, pp. 117–132, Apr. 2003.
- [9] E. J. Hughes, "Evolutionary many-objective optimisation: Many once or one many?" in *Proc. IEEE CEC-2005*, pp. 222–227.
- [10] Q. Zhang and H. Li, "MOEA/D: A multiobjective evolutionary algorithm based on decomposition," *IEEE Trans. Evol. Comput.*, vol. 11, no. 6, pp. 712–731, Dec. 2007.
- [11] D. K. Saxena, J. A. Duro, A. Tiwari, K. Deb, and Q. Zhang, "Objective reduction in many-objective optimization: Linear and nonlinear algorithms," *IEEE Trans. Evol. Comput.*, vol. 17, no. 1, pp. 77–99, 2013.
- [12] J. A. López and C. A. Coello Coello, "Some techniques to deal with many-objective problems," in *Proc. 11th Annu. Companion Genet. Evol. Comput. Conf.*, 2009, pp. 2693–2696.
- [13] H. Ishibuchi, N. Tsukamoto, and Y. Nojima, "Evolutionary many-objective optimization: A short review," in *Proc. CEC-2008*, pp. 2424–2431.
- [14] K. Sindhy, K. Miettinen, and K. Deb, "A hybrid framework for evolutionary multi-objective optimization," *IEEE Trans. Evol. Comput.*, vol. 17, no. 4, pp. 495–511, 2013.
- [15] H. Nakayama, K. Kaneshige, S. Takemoto, and Y. Watada, "An application of a multiobjective programming technique to construction accuracy control of cable-stayed bridges," *Eur. J. Oper. Res.*, vol. 87, no. 3, pp. 731–738, Dec. 1995.
- [16] M. Garza-Fabre, G. T. Pulido, and C. A. Coello Coello, "Ranking methods for many-objective optimization," in *Proc. MICAI-2009*, pp. 633–645.
- [17] V. Chankong and Y. Y. Haimes, *Multiobjective Decision Making Theory and Methodology*. New York, NY, USA: North-Holland, 1983.
- [18] C. M. Fonseca, L. Paquete, and M. López-Ibáñez, "An improved dimension sweep algorithm for the hypervolume indicator," in *Proc. CEC'06*, pp. 1157–1163.
- [19] L. While, P. Hingston, L. Barone, and S. Huband, "A faster algorithm for calculating hypervolume," *IEEE Trans. Evol. Comput.*, vol. 10, no. 1, pp. 29–38, Feb. 2006.
- [20] K. Deb, J. Sundar, N. Uday, and S. Chaudhuri, "Reference point based multiobjective optimization using evolutionary algorithms," *Int. J. Comput. Intell. Res.*, vol. 2, no. 6, pp. 273–286, 2006.
- [21] K. Deb and A. Kumar, "Interactive evolutionary multi-objective optimization and decision-making using reference direction method," in *Proc. GECCO-2007*, pp. 781–788.
- [22] K. Deb and A. Kumar, "Light beam search based multi-objective optimization using evolutionary algorithms," in *Proc. CEC-07*, pp. 2125–2132.
- [23] U. K. Wickramasinghe and X. Li, "A distance metric for evolutionary many-objective optimization algorithms using user-preferences," in *Proc. AI-2009*, LNAI 5866, pp. 443–453.
- [24] D. Brockhoff and E. Zitzler, "Dimensionality reduction in multiobjective optimization: The minimum objective subset problem," in *Proc. Oper. Res.*, 2007, pp. 423–429.
- [25] H. K. Singh, A. Isaacs, and T. Ray, "A Pareto corner search evolutionary algorithm and dimensionality reduction in many-objective optimization problems," *IEEE Trans. Evol. Comput.*, vol. 15, no. 4, pp. 539–556, Aug. 2011.
- [26] M. Laumanns, L. Thiele, K. Deb, and E. Zitzler, "Combining convergence and diversity in evolutionary multi-objective optimization," *Evol. Comput.*, vol. 10, no. 3, pp. 263–282, 2002.
- [27] D. Hadka and P. Reed, "Diagnostic assessment of search controls and failure modes in many-objective evolutionary optimization," *Evol. Comput. J.*, 2012, vol. 20, no. 3, pp. 423–452.
- [28] K. Deb and R. B. Agrawal, "Simulated binary crossover for continuous search space," *Complex Syst.*, vol. 9, no. 2, pp. 115–148, 1995.
- [29] M. Farina and P. Amato, "A fuzzy definition of optimality for many-criteria decision-making and optimization problems," *IEEE Trans. Syst., Man, Cybern.*, vol. 34, no. 3, pp. 315–326, May 2004.
- [30] X. Zou, Y. Chen, M. Liu, and L. Kang, "A new evolutionary algorithm for solving many-objective optimization problems," *IEEE Trans. Syst., Man, Cybern. B, Cybern.*, vol. 38, no. 5, pp. 1402–1412, Oct. 2008.
- [31] H. Aguirre and K. Tanaka, "Many-objective optimization by space partitioning and adaptive epsilon-ranking on MNK-landscapes," in *Proc. 5th EMO*, LNCS 5467. 2009, pp. 407–422.
- [32] H. Sato, H. E. Aguirre, and K. Tanaka, "Pareto partial dominance MOEA in many-objective optimization," in *Proc. CEC-2010*, pp. 1–8.
- [33] K. Miettinen, *Nonlinear Multiobjective Optimization*. Boston, MA, USA: Kluwer, 1999.
- [34] J. Branke, T. Kaußler, and H. Schmeck, "Guidance in evolutionary multi-objective optimization," *Advances Eng. Softw.*, vol. 32, no. 6, pp. 499–507, Jun. 2001.
- [35] G. Eichfelder, "Optimal elements in vector optimization with a variable ordering structure," *J. Optimization Theory Appl.*, vol. 151, no. 2, pp. 217–240, 2011.
- [36] K. Deb and H. Jain, "Handling many-objective problems using an improved NSGA-II procedure," in *Proc. WCCI-2012*, pp. 1–8.
- [37] Q. Zhang, H. Li, D. Maringer, and E. Tsang, "MOEA/D with NBI-style Tchebycheff approach for portfolio management," in *Proc. IEEE CEC*, pp. 1–8, 2010.
- [38] A. Zhou, Q. Zhang, and Y. Jin, "Approximating the set of Pareto optimal solutions in both the decision and objective spaces by an estimation of distribution algorithm," *IEEE Trans. Evol. Comput.*, vol. 13, no. 5, pp. 1167–1189, Oct. 2009.
- [39] R. C. Purshouse and P. J. Fleming, "On the evolutionary optimization of many conflicting objectives," *IEEE Trans. Evol. Comput.*, vol. 11, no. 6, pp. 770–784, Dec. 2007.
- [40] S. F. Adra and P. J. Fleming, "Diversity management in evolutionary many-objective optimization," *IEEE Trans. Evol. Comput.*, vol. 15, no. 2, pp. 183–195, Apr. 2011.
- [41] M. Köppen and K. Yoshida, "Substitute distance assignments in NSGA-II for handling many-objective optimization problems," in *Proc. EMO*, LNCS 4403. 2007 pp. 727–741.
- [42] D. Hadka and P. Reed, "Borg: An auto-adaptive many-objective evolutionary computing framework," *Evol. Comput.*, vol. 21, no. 2, pp. 231–259, 2013.
- [43] J. Bader and E. Zitzler, "Hype: An algorithm for fast hypervolume-based many-objective optimization," *Evol. Comput. J.*, vol. 19, no. 1, pp. 45–76, 2011.
- [44] J. Bader, K. Deb, and E. Zitzler, "Faster hypervolume-based search using Monte Carlo sampling," in *Proc. MCDM 2008*, 2010, pp. 313–326.
- [45] L. Bradstreet, L. While, and L. Barone, "A fast incremental hypervolume algorithm," *IEEE Trans. Evol. Comput.*, vol. 12, no. 6, pp. 714–723, Dec. 2008.
- [46] H. Li and Q. Zhang, "Multiobjective optimization problems with complicated Pareto sets, MOEA/D and NSGA-II," *IEEE Trans. Evol. Comput.*, vol. 12, no. 2, pp. 284–302, Apr. 2009.
- [47] Q. Zhang, A. Zhou, S. Z. Zhao, P. N. Suganthan, W. Liu, and S. Tiwari, "Multiobjective optimization test instances for the CEC-2009 special session and competition," Nanyang Technol. Univ., Singapore, Tech. Rep., 2008. <http://www.ntu.edu.sg/home/epnsugan/>.
- [48] I. Das and J. Dennis, "Normal-boundary intersection: A new method for generating the Pareto surface in nonlinear multicriteria optimization problems," *SIAM J. Optimization*, vol. 8, no. 3, pp. 631–657, 1998.

- [49] H. T. Kung, F. Luccio, and F. P. Preparata, "On finding the maxima of a set of vectors," *J. Assoc. Comput. Mach.*, vol. 22, no. 4, pp. 469–476, 1975.
- [50] Q. Zhang. (2012, Mar.). *MOEA/D Homepage* [Online]. Available: <http://dces.essex.ac.uk/staff/zhang/webofmoad.htm>
- [51] D. V. Veldhuizen and G. B. Lamont, "Multiobjective evolutionary algorithm research: A history and analysis," Dept. Electr. Comput. Eng., Air Force Inst. Technol., Dayton, OH, USA, Tech. Rep. TR-98-03, 1998.
- [52] H. Jain and K. Deb, "An evolutionary many-objective optimization algorithm using reference-point-based nondominated sorting approach, part II: handling constraints and extending to an adaptive approach," *IEEE Trans. Evol. Comput.*, vol. 18, no. 4, pp. 602–622, Aug. 2014.
- [53] K. Deb, L. Thiele, M. Laumanns, and E. Zitzler, "Scalable test problems for evolutionary multi-objective optimization," in *Evolutionary Multi-objective Optimization*, A. Abraham, L. Jain, and R. Goldberg, Eds. London, U.K.: Springer-Verlag, 2005, pp. 105–145.
- [54] K. Deb, K. Miettinen, and S. Chaudhuri, "Toward an estimation of nadir objective vector using a hybrid of evolutionary and local search approaches," *IEEE Trans. Evol. Comput.*, vol. 14, no. 6, pp. 821–841, 2010.
- [55] X. Liao, Q. Li, W. Zhang, and X. Yang, "Multiobjective optimization for crash safety design of vehicle using stepwise regression model," *Structural Multidisciplinary Optimization*, vol. 35, no. 6, pp. 561–569, 2008.
- [56] A. P. Wierzbicki, "The use of reference objectives in multiobjective optimization," in *Multiple Criteria Decision Making Theory and Applications*, G. Fandel and T. Gal, Eds. Berlin: Springer-Verlag, 1980, pp. 468–486.
- [57] K. Deb, S. Gupta, D. Daum, J. Branke, A. Mall, and D. Padmanabhan, "Reliability-based optimization using evolutionary algorithms," *IEEE Trans. Evol. Comput.*, vol. 13, no. 5, pp. 1054–1074, Oct. 2009.
- [58] J. D. Knowles and D. W. Corne, "Quantifying the effects of objective space dimension in evolutionary multiobjective optimization," in *Proc. 4th Int. Conf. Evol. Multi-Criterion Optimization*, 2007, pp. 757–771.
- [59] D. W. Corne, N. R. Jerram, J. D. Knowles, and M. J. Oates, "PESA-II: Region-based selection in evolutionary multiobjective optimization," in *Proc. GECCO-2001*, pp. 283–290.
- [60] M. Laumanns, G. Rudolph, and H. P. Schwefel, "A spatial predator-prey approach to multi-objective optimization: A preliminary study," in *Proc. Parallel Problem Solving From Nature V*, 1998, pp. 241–249.
- [61] K. Deb, M. Mohan, and S. Mishra, "Toward a quick computation of well spread Pareto-optimal solutions," in *Proc. EMO-03*, LNCS 2632, pp. 222–236.
- [62] H. Ishibuchi and T. Murata, "A multi-objective genetic local search algorithm and its application to flowshop scheduling," *IEEE Trans. Syst., Man, Cybern. C, Appl. Rev.*, vol. 28, no. 3, pp. 392–403, Aug. 1998.
- [63] A. Jaszkiewicz, "Genetic local search for multiple objective combinatorial optimization," *Eur. J. Oper. Res.*, vol. 137, no. 1, pp. 50–71, 2002.



Kalyanmoy Deb (F'12) is the Koenig Endowed Chair Professor with the Department of Electrical and Computer Engineering, Michigan State University, East Lansing, MI, USA. He has written two textbooks on optimization and more than 350 international journal and conference research papers. His research interests include evolutionary optimization algorithms and their applications in optimization and machine learning.

Mr. Deb was awarded a honorary doctorate degree from University of Jyvaskyla, Finland in 2013, the Infosys Prize in 2012, the TWAS Prize in Engineering Sciences in 2012, the CajAstur Mamdani Prize in 2011, the JC Bose National Fellowship in 2011, the Distinguished Alumni Award from IIT Kharagpur in 2011, the Edgeworth-Pareto Award in 2008, the Shanti Swarup Bhatnagar Prize in Engineering Sciences in 2005, and the Thomson Citation Laureate Award from Thompson Reuters.

He is on the Editorial Board of 20 major international journals, including *IEEE TRANSACTIONS ON EVOLUTIONARY COMPUTATION*.



Himanshu Jain is currently pursuing the Ph.D. degree in the Department of Computer Science and Engineering at the Indian Institute of Technology Delhi. He received the bachelor's and master's degree in mechanical engineering from the Indian Institute of Technology Kanpur, in 2012.

He was a member of the Kanpur Genetic Algorithms Laboratory (KanGAL), in 2009. His current research interests include evolutionary computation and machine learning.